



Norwegian University of
Science and Technology

Analyzes of Solar Chimney Design

Elias Paez Ortega

Master's Thesis

Submission date: July 2011

Supervisor: Per Olaf Tjelflaat, EPT

Norwegian University
of Science and Technology
NTNU

Department of Energy
and Process Engineering

EPT-M-2011-

MASTER THESIS

for

Stud.techn. Elias Páez Ortega
Spring 2011

Analyzes of Solar Chimney Design

Analyse av design for solskorstein

Background and objective.

In the search for building installations that use less electricity to work, and where noise generation is avoided, the solar chimney may be a good choice for buildings with natural and hybrid ventilation.

The present study aims to investigate the basic principles of solar chimneys and to test and improve the design of a solar chimney installed in the EPT lab.

The following should be considered in the project work:

- 1 A survey of solar chimney principles and of differences in design and application.
- 2 An experimental assessment of the solar chimney installation in the EPT-lab.
- 3 CFD- simulation of a basic solar chimney design and of the solar chimney in the EPT lab.
- 4 Comparison and discussion of results. Suggestions for improved solar chimney design.

Within 14 days of receiving the written text on the diploma thesis, the candidate shall submit a research plan for his project to the department.

When the thesis is evaluated, emphasis is put on processing of the results, and that they are presented in tabular and/or graphic form in a clear manner, and that they are analyzed carefully.

The thesis should be formulated as a research report with summary both in English and Norwegian, conclusion, literature references, table of contents etc. During the preparation of the text, the candidate should make an effort to produce a well-structured and easily readable report. In order to ease the evaluation of the thesis, it is important that the cross-references are correct. In the making of the report, strong emphasis should be placed on both a thorough discussion of the results and an orderly presentation.

The candidate is requested to initiate and keep close contact with his/her academic supervisor(s) throughout the working period. The candidate must follow the rules and regulations of NTNU as well as passive directions given by the Department of Energy and Process Engineering.

Pursuant to “Regulations concerning the supplementary provisions to the technology study program/Master of Science” at NTNU §20, the Department reserves the permission to utilize all the results and data for teaching and research purposes as well as in future publications.

One – 1 complete original of the thesis shall be submitted to the authority that handed out the set subject. (A short summary including the author’s name and the title of the thesis should also be submitted, for use as reference in journals (max. 1 page with double spacing)).

Two – 2 – copies of the thesis shall be submitted to the Department. Upon request, additional copies shall be submitted directly to research advisors/companies. A CD-ROM (Word format or corresponding) containing the thesis, and including the short summary, must also be submitted to the Department of Energy and Process Engineering

Department of Energy and Process Engineering, 17. January 2011

Olav Bolland

Department Manager

Per Olaf Tjelflaat

Academic Supervisor

Abstract

The aim of this work is to study the solar chimney installed in the EPT-lab of the NTNU. The work starts with the development of a CFD model of the solar chimney and comparing with the experimental data, showing a good accuracy of the CFD results. The CFD model is used to compare three types of solar chimneys for different heights and width; obtained that the chimney installed in the EPT-lab gets higher flow rates in the most of the cases. The CFD model shows a uniform temperature and velocity inside the chimney that allows developing a simple physical model of the chimney, which gives a good precision of results. Finally a simplification of the solar chimney and other systems installed in a building is simulated and also is developed another physical model for this kind of building, giving an idea of the behavior of this solar house in diverse conditions.

Contents

Abstract.....	III
1 Introduction.....	1—1
2 Theory.....	2—2
2.1 Fluid dynamics.....	2—2
2.1.1 Bernoulli equation.....	2—3
2.1.2 Boundary layer.....	2—5
2.1.3 Computational fluid dynamics.....	2—7
2.2 Chimney.....	2—11
2.2.1 Solar Chimney.....	2—12
3 Method.....	3—16
3.1 Experimental results.....	3—16
3.2 Development of CFD model.....	3—17
3.2.1 Boundary conditions.....	3—18
3.2.2 Chimney CFD model.....	3—25
3.2.3 Grid.....	3—28
3.2.4 Radiation model.....	3—29
3.2.5 Turbulence model.....	3—29
3.2.6 Results.....	3—33
3.3 Simplification of the model.....	3—36
3.3.1 Setting.....	3—36
3.4 Comparison different solar chimneys types.....	3—37
3.4.1 Results.....	3—39
3.5 Performance of the solar chimney.....	3—41
3.5.1 Theoretical equation.....	3—41
3.5.2 Validation of the theoretical equation.....	3—42
3.5.3 Pressure Vs Flow rate.....	3—45
3.5.4 Study of the control valve.....	3—48
4 Behavior of a building with a solar chimney.....	4—51
4.1 House model.....	4—51
4.2 Effect of difference of temperatures.....	4—52

4.3	Effect of the height of the chimney.....	4—54
4.4	Effect of wind	4—55
4.4.1	Wind velocity	4—55
4.4.2	Pressure coefficient (Cp)	4—56
4.5	Effect of a heat recovery.....	4—57
5	Further work.....	5—61
6	Conclusion	6—62
7	References.....	7—63
Appendix 1	- 1 -
	Pressure Loss Coefficients and Moody Diagram.....	- 1 -
Appendix 2	- 4 -
	Window data	- 4 -
Appendix 3	- 5 -
	Solar Chimney EPT-lab	- 5 -
Appendix 4	- 8 -
	CFD Solar Chimney Model	- 8 -

Figures

Figur 2-1 Boundary layer on flat plane.....	2—5
Figur 2-2 Turbulent boundary layer on flat plane	2—5
Figur 2-3 Profile of a turbulent boundary layer.....	2—6
Figur 2-4 Thermal boundary layer. Number of Prandtl	2—7
Figur 2-5 Chimney effect.....	2—11
Figur 2-6 Solar chimney in the EPT-lab	2—13
Figur 2-7 Chimney type Tånga School.....	2—14
Figur 2-8 Standard solar chimney	2—15
Figur 3-1 Experimental results of velocity.....	3—16
Figur 3-2 Residuals configuration 1	3—19
Figur 3-3 Temperatures configuration 1(K).....	3—20
Figur 3-4 Residuals configuration 2	3—21
Figur 3-5 Residuals configuration 3	3—21
Figur 3-6 Temperatures configuration 3	3—22
Figur 3-7 Residuals configuration 4	3—22
Figur 3-8 Residual configuration 5.....	3—23
Figur 3-9 Temperatures configuration 5	3—23
Figur 3-10 Residuals configuration 6	3—24
Figur 3-11 Velocity configuration 6.....	3—25
Figur 3-12 Stream function inlet.....	3—26
Figur 3-13 Chimney inlet	3—26
Figur 3-14 Chimney CFD Model	3—27
Figur 3-15 Grid fins	3—28
Figur 3-16 Grid wall.....	3—28
Figur 3-17 Fin temperature. Different radiation models	3—29
Figur 3-18 Velocity profile in the outlet (first simulation)	3—31
Figur 3-19 Profiles of turbulent dissipation rate	3—31
Figur 3-20 Velocity profiles h=3m.....	3—32
Figur 3-21 Velocity profiles h=4,15m	3—33
Figur 3-22 velocity contours 3m and 4,15m.....	3—34
Figur 3-23 Temperature contours 3m and 4,15m	3—34
Figur 3-24 Temperatures profiles in chimney outlet	3—35
Figur 3-25 Temperature contour of the collector	3—35
Figur 3-26 Simplified model	3—36
Figur 3-27 Models of the types of solar chimney	3—38
Figur 3-28 Temperatures in type 3	3—39
Figur 3-29 Mass flow Vs Width.....	3—40
Figur 3-30 Mass flow Vs Height	3—40
Figur 3-31 q Vs Q (H=cte)	3—43

Figur 3-32 Temperature Vs Q (H=cte)	3—43
Figur 3-33 q Vs H (Q=cte)	3—43
Figur 3-34 Temperature Vs H (Q=cte)	3—43
Figur 3-35 Efficiency (%) Vs Q	3—44
Figur 3-36 Efficiency (%) Vs H	3—44
Figur 3-37 Behavior of the control valve.....	3—46
Figur 3-38 Hydrostatic pressure from the chimney	3—47
Figur 3-39 Pressure Vs Flow rate	3—47
Figur 3-40 Curves of different types of fan	3—48
Figur 3-41 K Vs % opening	3—49
Figur 3-42 % flow rate Vs % opening	3—50
Figur 3-43 Control valve flow characteristics	3—50
Figur 3-44 Effect of authority in a linear valve	3—50
Figur 4-1 House model	4—51
Figur 4-2 Flow rate Vs difference of temperatures	4—53
Figur 4-3 Flow rate Vs $dT > 0$	4—54
Figur 4-4 Solar efficiency Vs difference of temperature	4—54
Figur 4-5 Flow rate vs. dT (various height)	4—55
Figur 4-6 Flow rate Vs dT (wind velocity)	4—56
Figur 4-7 rate Vs dT (C_p).....	4—57
Figur 4-8 Flow rate Vs dT (heat recovery)	4—58
Figur 4-9 solar efficiency Vs dT (heat recovery)	4—59
Figur 4-10 Flow rate Vs $dT > 0$ (heat recovery)	4—59
Figur 4-11 Flow rate Vs dT (heat pipe recovery)	4—60

Tables

Table 1 Experimental results	3—16
Table 2 Properties of the flow	3—17
Table 3 Comparison of velocity. Experimental Vs CFD	3—33
Table 4 Difference Coefficient of pressure drop	3—37

1 Introduction

The equipments, materials or human activity increase the pollutant concentration inside the building, which affects to the indoor air quality. Pollutant concentration can affect human health and productivity, which makes necessary their removal. Traditionally the ventilation replaces the indoor air for outdoor air, which has better quality.

The different modes of promoting air exchange are mechanical ventilation, which allows controlling the flow rate all the moment, their quality and temperature; and natural ventilation, which has less maintenance, makes less noise and does not use electric energy to move the air.

The solar chimney is a system that uses the solar radiation to move the air, improving the natural ventilation and in some cases providing fresh air for the building. Many works were carried out the last two decades demonstrating the advantages of solar chimney, for example the difference of a traditional chimney and a solar chimney [1], the temperature impact of a solar chimney [2] or their benefit in hybrid ventilation systems [3]. Other works focus in the design of the solar chimney as the height, width or angle of tilt, using in the most of the cases CFD tools to carry out the simulations or experiments and developments physical and mathematical models for a solar chimney [1, 4-7]. Also other works centers in the study of a building with a solar chimney and other ventilation systems as a cooling cavity [8], Trombe walls [9] or heat recovery [4]. All these studies shows the viability of the this system and nowadays one can see that new buildings start to install solar chimneys, like the Tånga School in Falkenberg Sweden [10].

The aim of this thesis is the new design of solar chimney made in the EPT-lab of the Norwegian University of Science and Technology, which pretends to demonstrate the advantages against others chimney's design, develop a physical model of the chimney and study the effect of a building with this solar chimney.

2 Theory

The aim of this chapter is to make an introduction of the theory, concepts and principles used in this Thesis.

2.1 Fluid dynamics

The Navier-Stokes equations describe the motion of a fluid substance:

- Continuity

$$\frac{\partial \rho}{\partial t} + \nabla(\rho \bar{u}) = 0 \quad 2.1$$

- Momentum

$$\rho \frac{\partial \bar{u}}{\partial t} + \rho \bar{u} \nabla(\bar{u}) = -\nabla p + \frac{\mu}{\rho} \nabla^2 \bar{u} + \rho \bar{f}_m \quad 2.2$$

- Energy

$$\rho \frac{\partial c_p T}{\partial t} + \rho \bar{u} \nabla(c_p T) = -p \nabla \bar{u} + \bar{\tau} : \nabla \bar{u} + \nabla(k \nabla T) \quad 2.3$$

These equations do not have an analytic solution; therefore usually it used simplification of these ones to achieve an approximate solution. The dimensionless number is used to carry out these simplifications, as the Reynolds number or the Rayleigh number.

The Reynolds number gives a measure of the ratio of inertial forces to viscous forces and consequently quantifies the relative importance of these two types of forces for given flow conditions.

$$Re = \frac{\rho U D}{\mu} \quad 2.4$$

When this number is high ($Re \gg 1$) the viscous forces can be neglected. Also when $Re < 2300$ in ducts a laminar flow occurs and for $Re > 4000$ the flow is turbulent.

The Rayleigh measures the importance of buoyancy driven flow). When the Rayleigh number is below the critical value for that fluid, heat transfer is primarily in the form of conduction; when it exceeds the critical value, heat transfer is primarily in the form of convection.

$$Ra = \frac{g\beta\Delta T c_p \rho^2 L^3}{\mu k} \quad 2.5$$

Besides, in a pure natural convection the Rayleigh number measures the strength of the buoyancy-induced flow. When $Ra < 10^8$ indicates an induced laminar flow and a transition to turbulent flow among $10^8 < Ra < 10^{10}$.

2.1.1 Bernoulli equation

The Bernoulli equation is the result of the simplification of the Navier-Stokes equations assuming an inviscid fluid ($Re \gg 1$).

$$\frac{1}{2}\rho v^2 + P_s = cte = P_t \quad 2.6$$

This means, if the velocity increases, the static pressure has to decrease.

This equation can be completed summing the effects of gravity and a turbo machine.

$$\frac{1}{2}\rho v^2 + P_s + \rho gh + \Delta P_{fan} = P_t \quad 2.7$$

2.1.1.1 Pressure loss

In every duct system are present pressure losses due to the circulation of a fluid inside a duct (primary pressure loss) and caused by additional components as a valve, contractions or inlets (secondary pressure loss). These pressure losses can be incorporated in the Bernoulli equation:

$$\frac{1}{2}\rho v^2 + P_s + \rho gh + \Delta P_{fan} = P_t + \frac{1}{2}\rho v^2 \sum K_{drop} \quad 2.8$$

The total coefficient of pressure drop ($\sum K_{drop}$) is the sum of the primary pressure loss and secondary pressure loss.

- Primary pressure loss

$$f\left(Re, \frac{\epsilon}{Dh}\right) \quad 2.9$$

$\frac{L}{Dh} = \text{length of the duct}$
 $Dh = \text{hydraulic diameter of the duct}$

$$f = \text{friction coefficient of Darcy}$$

$$\epsilon = \text{rugosity of the duct}$$

The friction coefficient of Darcy can be estimated with the Moody chart.

- The secondary pressure loss depends of the components of the system. Every component has its own coefficient of pressure loss, and in the most of the cases can be calculated with charts. In this thesis the secondary pressure are the inlet, outlet, nozzle and valve. All this components have a constant coefficient of pressure loss.

All the charts used in this thesis can be found in Appendix 1

2.1.1.2 Buoyancy and stack effect

Buoyancy is the force, along with the gravity, involved in the movement to upper positions of an object or fluid with less density than the fluid surrounding.

In ideal gases when the temperature increases, the density decrease, thus a movement between the cold and warm zones appears. This movement is knowledge as Stack effect [11]. The pressure difference of the stack effect is the next equation 2.10.

$$\Delta P_{stack} = gH\Delta\rho$$

$$\Delta P_{stack} = \rho gH \frac{\Delta T}{T_i} \quad \mathbf{2.10}$$

The problem of this driven force is that it connects the energy and momentum equations (equations 2.2 and 2.3) hindering the solution of the problem.

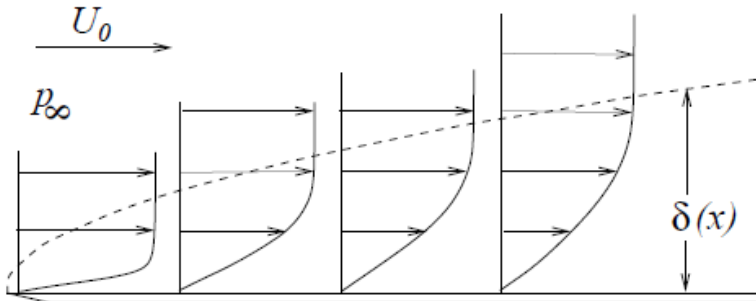
To get a faster solution usually is used the Boussinesq Model. This model treats the density as constant value in all the equations except in the buoyancy term of the momentum equation.

$$\rho = \rho_0(1 - \beta\Delta T) \rightarrow \beta\Delta T \ll 1 \quad \mathbf{2.11}$$

$$\Delta P_{buoyancy} = \rho gH\beta\Delta T \quad \mathbf{2.12}$$

2.1.2 Boundary layer

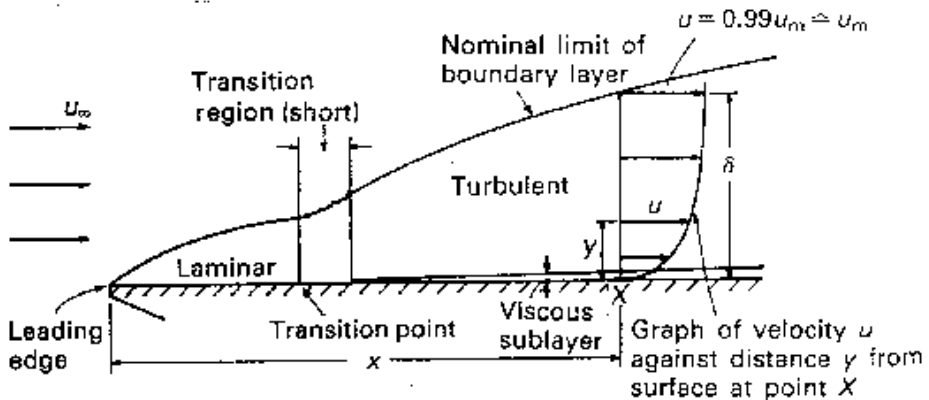
For flows with high Re , the effect of the viscosity is neglected, but areas close to walls, the viscosity has to take into account because this area in the most of the cases affect to the solution. This area is the boundary layer and its study is very important to understand the behavior of the solar chimney



Figur 2-1 Boundary layer on flat plane

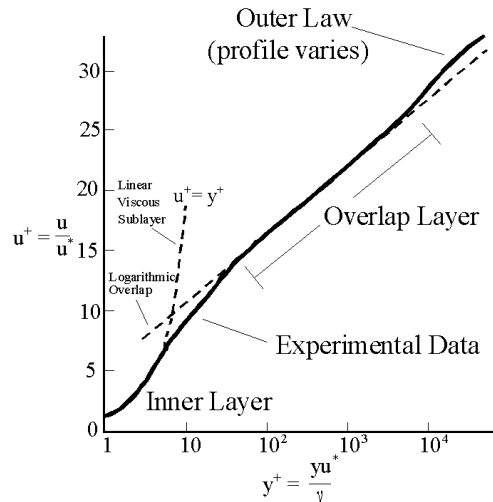
2.1.2.1 Turbulent boundary layer

As same happens in flows trough ducts, if the velocity or the length is enough high ($Re \gg 1$), the boundary layer can change from laminar to turbulent. In this case the layer is considerably more complex, at the same is coarser, and dissipates more energy; thus the friction is higher. Nevertheless the turbulent boundary layer moves the kinetic energy from the exterior to the interior, improving the heat transfer between the flow and wall.



Figur 2-2 Turbulent boundary layer on flat plane

The turbulent boundary layer can be divided into two zones: the zone of defect of velocities or outer law and zone near to the wall divided also in other two zones, the viscous sublayer or inner law and the logarithmic sublayer or overlap layer (Figur 2-3). This zone near the wall is very important to know the mesh resolution in CFD simulations.



Figur 2-3 Profile of a turbulent boundary layer

2.1.2.2 Thermal boundary layer

In general, the temperature of the flow T_{∞} usually does not agree with the temperature of the wall T_c . As same as the velocity boundary layer, a thermal boundary layer appears.

The study of the thermal boundary layer is important in the design of a solar chimney since this is involved in the heat transfer between the wall and the fluid and also in the stack effect.

The thickness of the thermal boundary layer depends of the number of Prandtl, defined as:

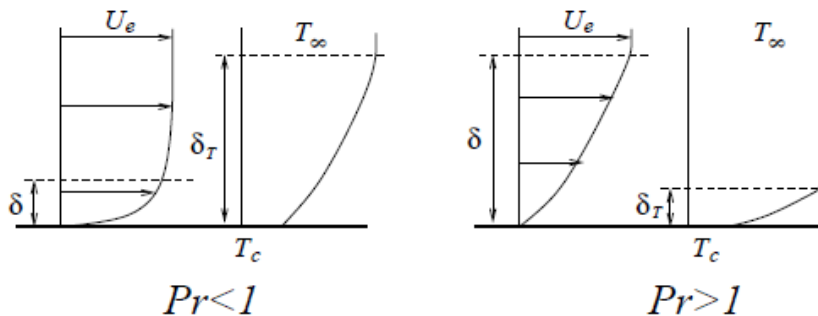
$$Pr = \frac{c_p \mu}{k} \quad 2.13$$

c_p = Specific heat

μ = Viscosity

k = Thermal conductivity

When this number is higher than one ($Pr > 1$) the thickness of the thermal boundary layer is higher than the velocity boundary layer and the opposite if $Pr < 1$. When Pr is near to one, the sizes of both boundary layers have the same order. Figur 2-4 shows this behavior.



Figur 2-4 Thermal boundary layer. Number of Prandtl

The thickness can be estimated with the following equation

$$\frac{\delta_T}{L} \sim \left\{ \begin{array}{ll} Pr^{-\frac{1}{2}} Re^{-\frac{1}{2}} & Pr < 1 \\ Pr^{-\frac{1}{3}} Re^{-\frac{1}{2}} & Pr > 1 \end{array} \right\} \quad 2.14$$

$\delta_T =$ Thickness of the thermal boundary layer

$L =$ Length of the wall

2.1.3 Computational fluid dynamics

Computational fluid dynamics (CFD) is a computer based tool design to solve a wide range of fluid mechanics problems. The CFD solves the three equations of fluid flow (continuity, momentum and energy) approximately. First the geometry of the model is discretized in thousand of cells and nodes; the state of one node is affected by the neighboring nodes and the boundary conditions.

The accuracy of the solution depends of many factors as the size of the cell, the number of iterations, the boundary conditions selected, the size of the domain, the models selected (turbulent, radiation or materials), the discretization used (first order, second order,...) and other factors. Thus a standard solution method does not exist and is necessary a deeply study of

the properties and conditions on each problem and in the mainly cases a validation with experimental results.

In this Master Thesis it have been used Fluent to simulate the fluid flow, since is one of the most development and used CFD programs.

2.1.3.1 RANS/ Turbulent models

When the $Re \gg 1$ the solution of the Navier-Stokes equations became unstable with small perturbations. These perturbations develop as the flow increases, leading to turbulence characterized for quick variation both spatial and temporal. Since these fluctuations can be of small scale and high frequency, they are too computationally expensive to simulate directly in the most of engineering calculations.

In the most of the cases a time-averaged solution for the magnitudes is enough. The equation of Reynolds Average Navier Stokes (RANS) is the result of decomposing the flow magnitudes (velocity, pressure, temperature...) in two, the average component and the fluctuating component.

$$a = \bar{a} + a' \quad 2.15$$

For example the momentum RANS equation is:

$$\rho \frac{\partial \bar{u}}{\partial t} + \rho \bar{u} \nabla(\bar{u}) = -\nabla \bar{p} + \frac{\mu}{\rho} \nabla^2 \bar{u} + \frac{1}{\rho} \nabla(-\rho \overline{u' u'}) + \rho \bar{f}_m \quad 2.16$$

As one can see, the modified equation contain a new unknown variable, $-\rho \overline{u' u'}$, Reynolds stresses tensor represents the effects of turbulence and must be modeled in order to close the equation. Thus turbulence models are designed to determine this variable in terms of known quantities and close the RANS equations.

$$-\rho \overline{u_i u_j} = \mu_t \left(\frac{\partial u_i}{\partial x_j} + \frac{\partial u_j}{\partial x_i} \right) - \frac{2}{3} \left(\rho k + \mu_t \frac{\partial u_k}{\partial x_k} \right) \delta_{ij} \quad 2.17$$

Equation 2.17 represents the Boussinesq hypothesis what introduce the new concept of turbulent viscosity μ_t (property of the flow). The concept of

turbulent viscosity reduces the computational cost. However it assumes μ_t is an isotropic scalar quantity, which is not strictly true.

The alternative is to solve transport equations for each of the terms in the Reynolds stress tensor, which means that five additional equations have to be solved in 2D and seven in 3D.

Unfortunately, the choice of the turbulent model is not the same for all kinds of problems. It is necessary to understand the capabilities and limitations of the models, besides other considerations such as the accuracy, the computational resources, time available and the class of problem. Fluent provides a wide range of turbulence models, but only five are taken into account in this Thesis.

- Standard k-e model

It is a semi-empirical model based on model transport equation for turbulent kinetic energy (k) and its dissipation rate (e).

$$\mu_t = \rho C_\mu \frac{k^2}{e} \quad 2.18$$

$$C_\mu = \text{constant}$$

The standard k-e model is the simplest “complete models” of turbulence. It assumes that the flow is fully turbulent and the molecular viscosity is negligible.

- Realizable k-e problem

The realizable k-e model is an improvement of the standard k-e problem. There are new formulations for the dissipation rate (e) and for the turbulent viscosity.

$$C_\mu = \frac{1}{A_0 + A_S \frac{U^* k}{e}} \quad 2.19$$

C_μ is no longer constant in this model.

The realizable k-e model predicts more accurately the spreading rate of both planar and round jets. Also it can be used in transition to turbulent flows.

Both models take into account the effect of the generation of k due to buoyancy.

- Transition k-kl- ω model
This model is used to predict boundary layer development and can be used in flows with the transition of the boundary layer from laminar to turbulent regime.
The disadvantage is that it resolves three transport equations increasing the computational cost.
- Transition SST model
It is a four transport equations model, which improves the accuracy of simulations with flows in low free-stream turbulence environments.
- Reynolds stress model (RSM)
This is the most complete turbulent model that one can find in Fluent. This model does not use the Boussinesq hypothesis, thus five transport equations are solved in this model. Usually the model gives more accurate results than the others in the mainly kind of flows. This model requires closure assumptions employed in the transport equations for the Reynolds stresses tensor.

2.1.3.2 Radiation models

In this section, it is going to describe the characteristic of the radiation models and not the theory behind, due to its long formulation and explanation.

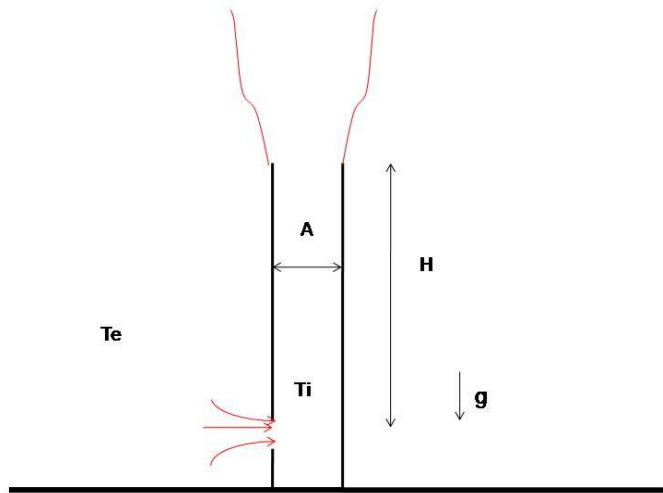
Fluent provides five radiations models, but only are going to take into account in the simulations of this Thesis.

- The P-1 model is a diffusion equation, which is one of the radiations who less computational resources use.
This model assumes gray radiation and that the all surfaces are diffuse. It will be a loss of accuracy if the optical thickness is small and also tends to over predict radiative fluxes from localized heat sources.
- The DO works with the entire range of optical thickness, with a computational cost moderate.
The model allows to work with non gray radiation and also with semi-transparent walls.

2.2 Chimney

A chimney is device usually used to remove the hot flue gas or smoke to the atmosphere. It uses the stack effect to induce the movement.

In buildings, the chimney also is used in natural ventilation, taking advantage of the differences of temperature between in-outside the building.



Figur 2-5 Chimney effect

Adding equation 2.8 and 2.10 in the condition of Figur 2-5:

$$\rho g H \frac{\Delta T}{T_i} = \frac{1}{2} \rho v^2 \sum K_{drop}$$

$$v = \sqrt{\frac{2gH \frac{\Delta T}{T_i}}{\sum K_{drop}}} \rightarrow Cd = \frac{1}{\sqrt{\sum K_{drop}}}$$

$$q = Cd \cdot A \sqrt{2gH \frac{T_i - T_e}{T_i}} \tag{2.20}$$

Equation 2.20 can be used to estimate the natural draught flow rate (q) assuming that the heat loss negligible.

2.2.1 Solar Chimney

A solar chimney is a kind chimney that uses the solar radiation to increase the temperature inside generating the stack effect to move the air. Usually it is used as a way to improve the natural ventilation for a building. Also it can be used to generate electrical energy, but in this cases the size it considerably bigger, for example the solar tower built in Manzanares, Spain was 195m high obtaining a maximum output power of 50 KW [12].

This Thesis is focus only in the solar chimney as a way to improve the natural ventilation.

2.2.1.1 Chimney types

There is not only one design for solar chimney. It depends of the latitude of the place, the height of the building, the solar collector or the materials.

Nowadays, the most widely used is that one that replaces part of the south facade for a glazing allowing, the solar radiation, to get inside the chimney.

This Thesis studies three types of solar chimney.

- **Type 1**

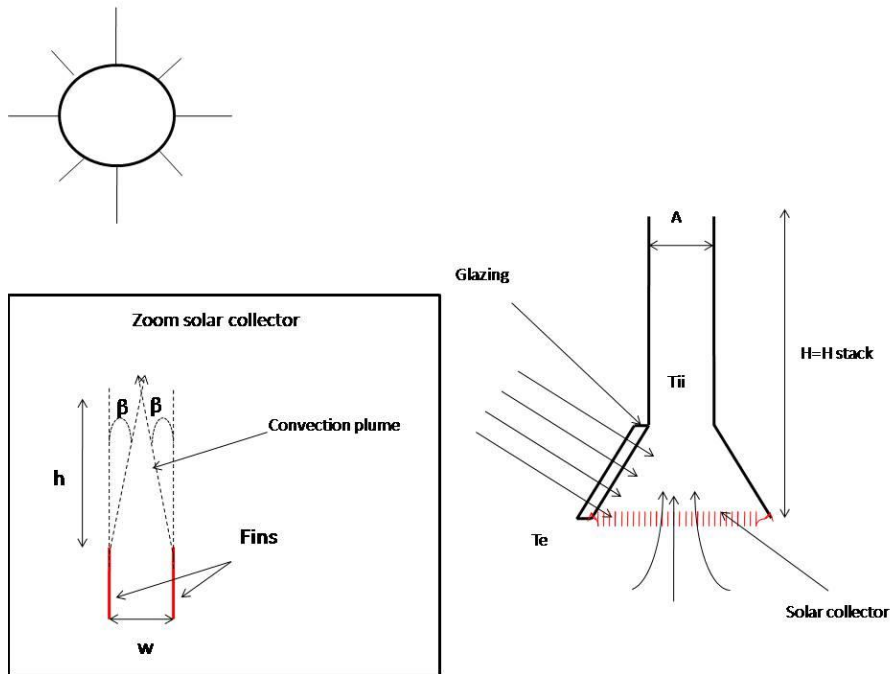
This solar chimney is installed in the EPT-lab for the Norwegian University of Science and Technology. This chimney is the base of this Thesis, because is a new type designed by this university in the project [13] and therefore not so much information about the behavior and characteristics can be found.

In Figur 2-6 one can see the operating principle of this chimney. The solar radiation passes through the glazing, situated in the down part of the south façade, and it is absorbed by the solar collector (in the bottom of the chimney). The solar collector is a high number of thin parallel metallic fins (33 in the EPT-lab); the fin receives the solar radiation, increasing the temperature of the surfaces, this generates a convection plume for each fin. The distance between two consecutive fins is relative small ($w=4,4\text{cm}$) and the angle from the centerline of the plume to the boundary is approximately $\beta=12.5^\circ$ [14]. Thus the distance where two consecutives plumes touch each other is:

$$h = \frac{w}{2 \cdot \tan \beta} = \frac{4,4}{2 \cdot \tan 12,5^\circ}$$

$$h = 9,92 \text{ cm} \quad \mathbf{2.21}$$

At this distance, one can consider a homogeneous temperature inside the chimney. Note that the height of the chimney is bigger (300cm) than “h”, therefore it is assumed that the height of the chimney and the height of the stack effect it is the same.



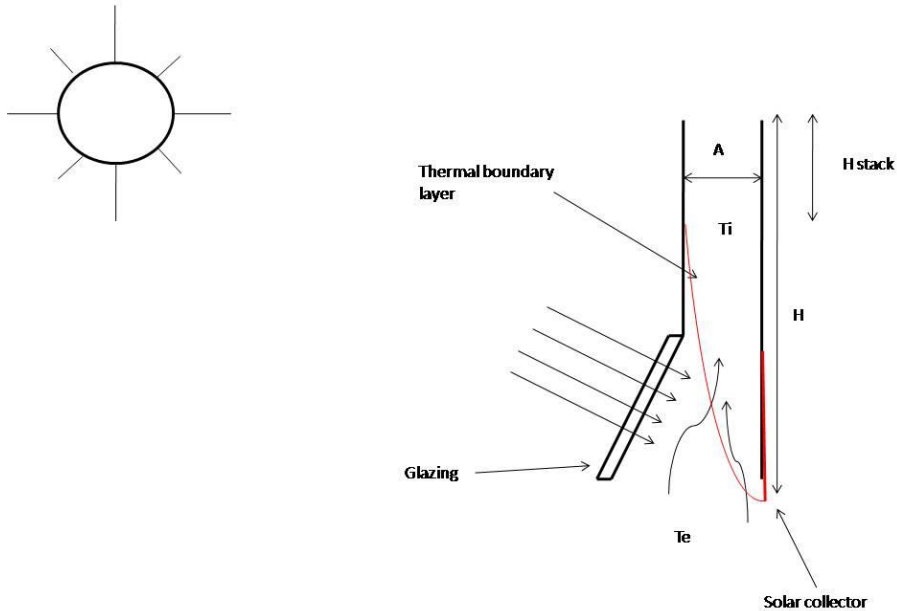
Figur 2-6 Solar chimney in the EPT-lab

- **Type 2**

This type of chimney is installed in the Tånga School in Falkenberg Sweden [10]. It is designed for cold climates (higher latitudes)

Like the type 1, this chimney changes the down part of the south wall for a glazing. The chimney is designed for cold climates (higher latitudes), that's why just a part of the south facade is a glass to minimize the heat loss trough the chimney, since this chimney also uses the stack effect of the building to improve natural ventilation.

The radiation cross the window and it is absorbed by the solar collector, but in this case it is the front wall, which is painted in black to improve the absorption of radiation (Figur 2-7). In this case the height of the chimney and the height of the stack there are not the same; as an approximation, the begging of stack effect's height can be calculated as the point where the thermal boundary layer touches the south wall.

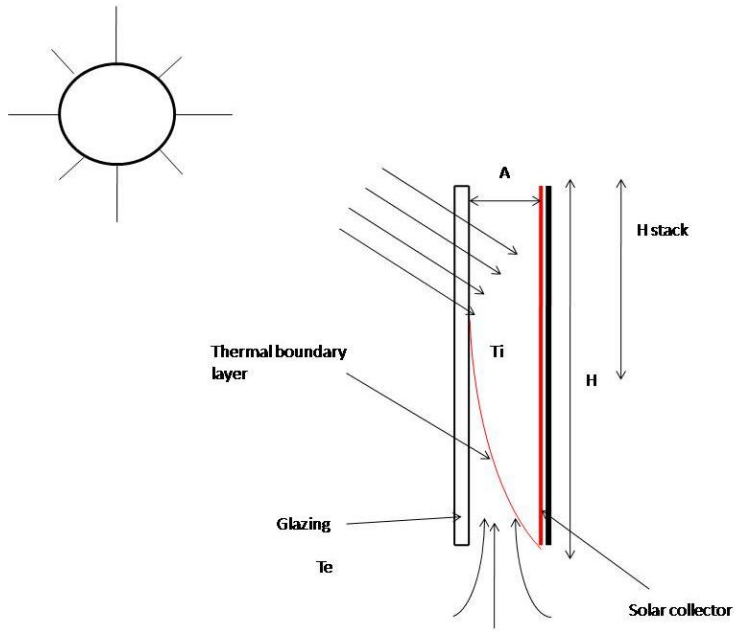


Figur 2-7 Chimney type Tånga School

- **Type3**

This kind of solar chimney is the most used and studied [1, 4, 8, 9]; also it is developed for warmer and tropical climates.

The design is very simple; the south wall is a glass allowing the radiation gets to the solar collector, which is the front wall, also painted in black (Figur 2-8). Like the type 2, the height of the stack effect defers from the height of the chimney; and can be calculated with the same conditions.



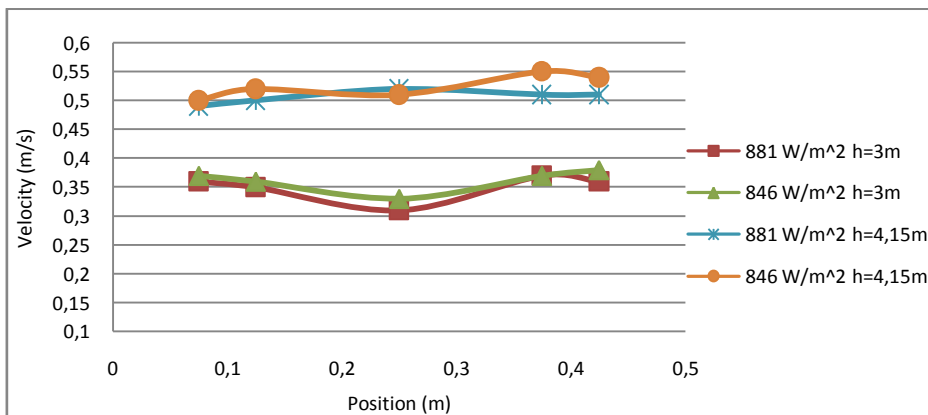
Figur 2-8 Standard solar chimney

3 Method

3.1 Experimental results

The basis of the development of the solar chimney's CFD model is the experimental results taken from the project "Development of Air solar Collector" [13]. In this project can be found velocity, temperature, height and radiation experimental data from the solar chimney studied in this thesis.

As the CFD model will be a 2-D model, only is necessary take the midplane data from the solar chimney. The results are showed in the next figure and table.



Figur 3-1 Experimental results of velocity

Radiation (W/m ²)	Velocity h=3m (m/s)	Velocity h=4,15m (m/s)
881,7	0,35	0,506
846,4	0,362	0,524

Table 1 Experimental results

Also the temperature increase in the surroundings of the collector is around $\Delta T \approx 2$ and 3 K.

3.2 Development of CDF model

The first step to build the CFD model is know the fluid field properties, as the Reynolds number or Rayleigh number to select the turbulence, radiation and fluid models

- Properties of the flow:

Name	Symbol	Value
Density	ρ	$1,225 \frac{kg}{m^3}$
Viscosity	μ	$1,7894 \cdot 10^{-5} \frac{kg}{m \cdot s}$
Specific heat	c_p	$1006,43 \frac{J}{kg \cdot K}$
Thermal conductivity	k	$0,0242 \frac{W}{m \cdot K}$
Thermal expansion coefficient	β	$0,00341 \frac{1}{K}$
Hydraulic diameter	D_h	$0,5 m$
Longitude (height)	L	$3 m$
Average velocity	U	$0,4 \frac{m}{s}$
Average difference of temperatures	ΔT	$2 K$
Gravity	g	$9,81 \frac{m}{s^2}$

Table 2 Properties of the flow

- Reynolds number:

$$Re = \frac{\rho U D_h}{\mu} = 13692 \quad 3.1$$

- Rayleigh number:

$$Ra = \frac{g \beta \Delta T c_p \rho^2 L^3}{\mu k} = 6,3 \cdot 10^9 \quad 3.2$$

- Boussinesq fluid model:

$$\beta \Delta T \approx 0,07 \ll 1 \quad 3.3$$

With these small differences of temperatures and the thermal expansion coefficient, one can assume a Boussinesq model

In brief, it is working in a transition- turbulent problem, where is possible to use the Boussinesq model for the buoyancy effects.

3.2.1 Boundary conditions

Have been studied six types of different configurations of boundary conditions, to find which of these ones obtains a better converge of the problem and less affect to the actual conditions.

In this case, has been used a simple model of a symmetric chimney, to reduce the time of simulations. The six different types of configurations are the following:

1. The limits of the model are walls with slip conditions and constant temperature
2. There is a velocity inlet of 0.5 m down in the left wall, outflow of 0.1 m in the left at the top wall and the rest is a wall with slip conditions. Both velocity inlet and wall have the same constant temperature.
3. The same as above, except that the velocity is in the top and the outflow in the bottom.
4. The bottom is a velocity inlet, the top is an outflow condition and the right side is a wall with slip conditions.
5. The same as above, except that the top is a pressure outlet condition.
6. The bottom is a pressure inlet condition, the top a pressure outlet and right side a wall with slip condition.

Where velocity inlet conditions are used has to be careful with the velocity magnitude. In this cases have been used the ratio of Grashof and Reynolds numbers:

$$\frac{Gr}{Re^2} = \frac{g\beta\Delta TL}{U^2} \quad 3.4$$

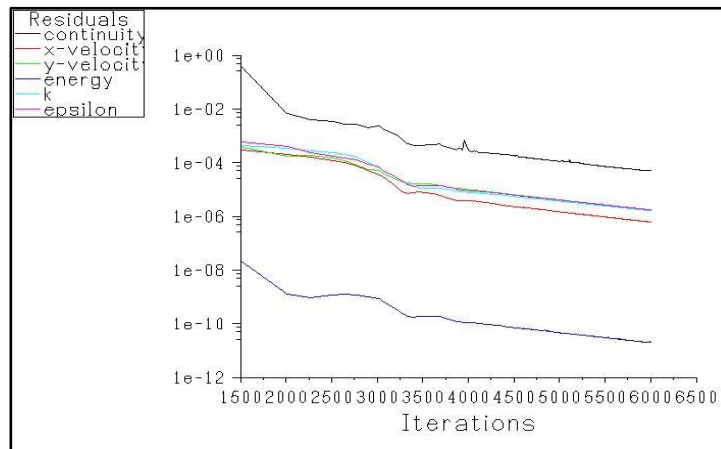
This number measures the importance of buoyancy forces in a mixed convection flow. When this number is bigger than unity, the buoyancy effects are stronger than the velocity inlet. To be sure that the velocity inlet

does not interfere in the buoyancy forces of the problem, has been select a ratio equal or bigger than 100, which corresponds a velocity of 0.01 m/s.

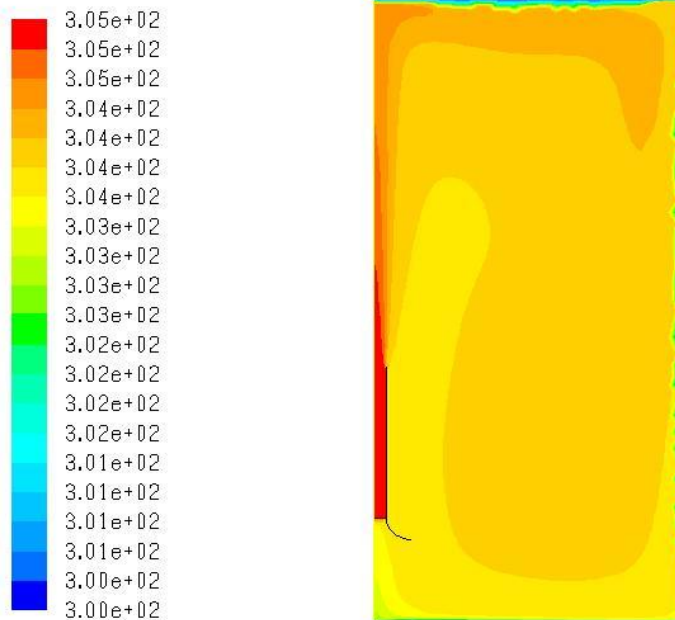
The model used in all the cases is the same and it is a symmetric chimney with a radiator boundary condition in the bottom of this one with a heat flux of 300 W/m^2 , the external temperature is 300 K (external walls and inlets) and the turbulence model is standard k-e with standard wall functions and thermal buoyancy effects.

- Configuration 1 does not have problems with the convergence as it shows in Figur 3-2, but take so many iterations to have a good value of residuals (more than 6000 iterations to have residual of continuity less than 10^{-4}).

On the other hand, if one checks the temperature's field in the model, one can see that the temperature in the fluid increases around 4°C more than the external walls (Figur 3-3), therefore this boundary condition does not satisfy the external temperature condition.

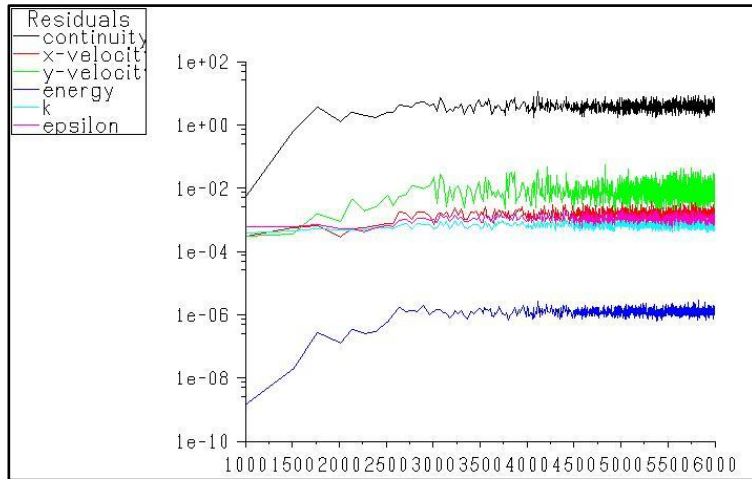


Figur 3-2 Residuals configuration 1



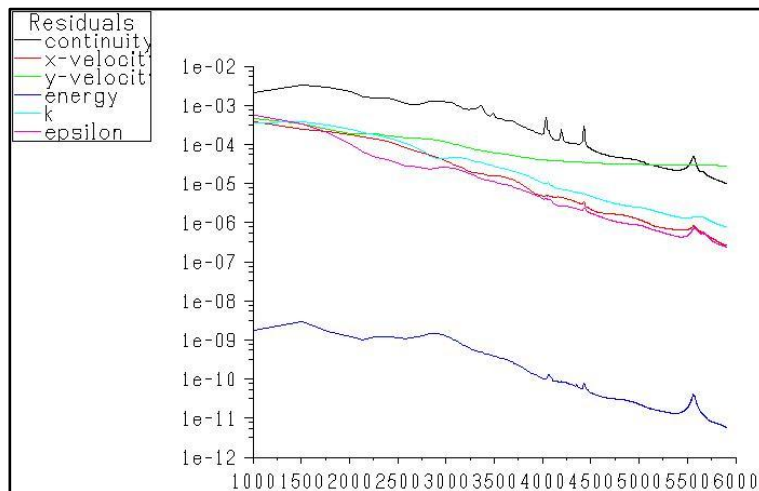
Figur 3-3 Temperatures configuration 1(K)

- The configuration 2 has an unstable solution as Figur 3-4 shows. The reason of this is that the outlet condition is not long enough to take all the heat of the radiator, then, the fluid in the model is warmer than the inlet flow. This fact makes that the boundary conditions are situated in the opposite direction of the natural flow, i.e. it has a cold flow inlet in the bottom and the out flow on the top, so it is forcing a cold flow goes up, when the normal is that the cold flow goes down. This conclusion motivated the next boundary condition.

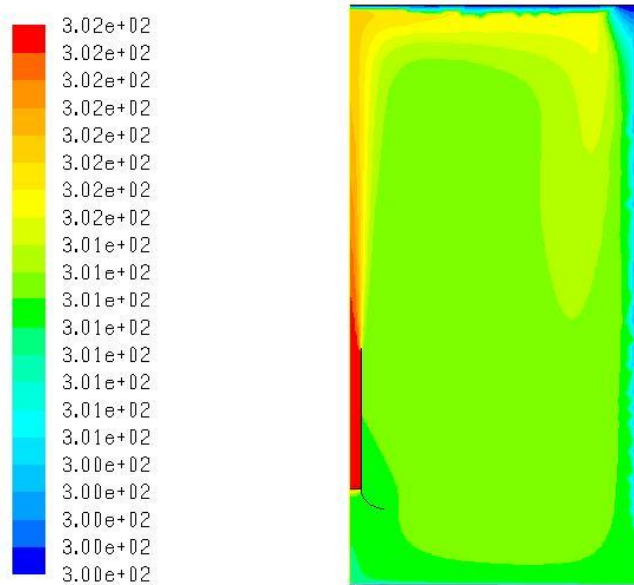


Figur 3-4 Residuals configuration 2

- The configuration 3 has a better convergence than the 1 (Figur 3-5), in less than 6000 iterations it has a residual continuity under 10^{-4} . Also, the configuration has the difference of temperatures between external and the fluid problem, but in this case is lower (Figur 3-6), around 2°C .

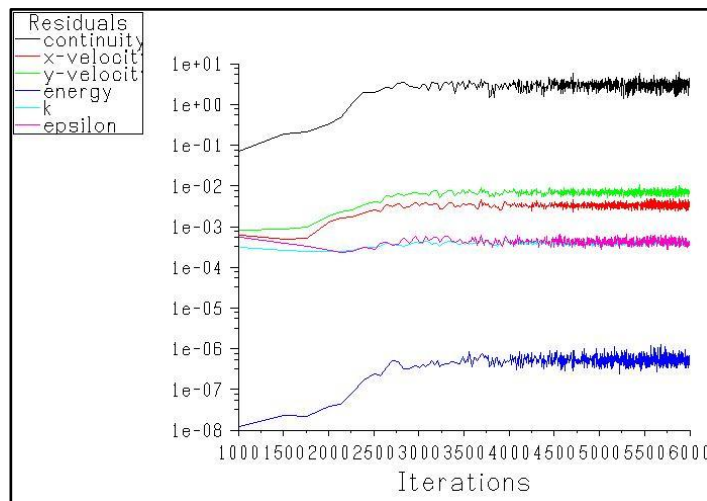


Figur 3-5 Residuals configuration 3



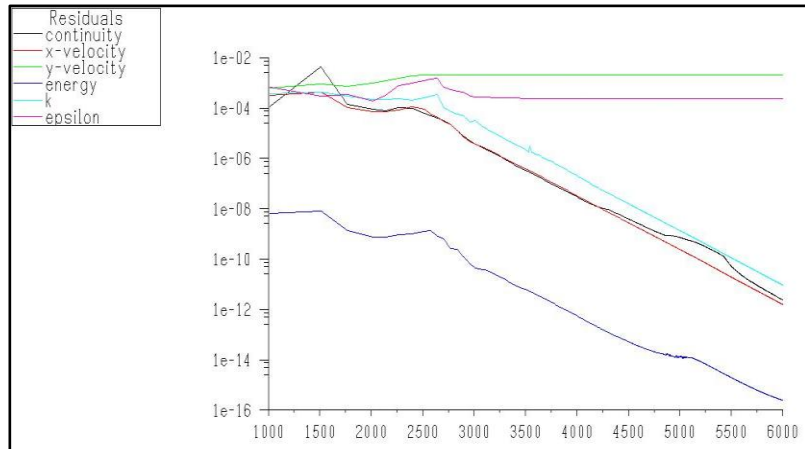
Figur 3-6 Temperatures configuration 3

- The configuration 4 is unstable (Figur 3-7), because in the outlet appears a reflow induced for the chimney's jet. The outlet condition has problems with inverse flow; the solution is change to a pressure outlet condition who can work with inverse flows, which it has been done in the configuration 5.



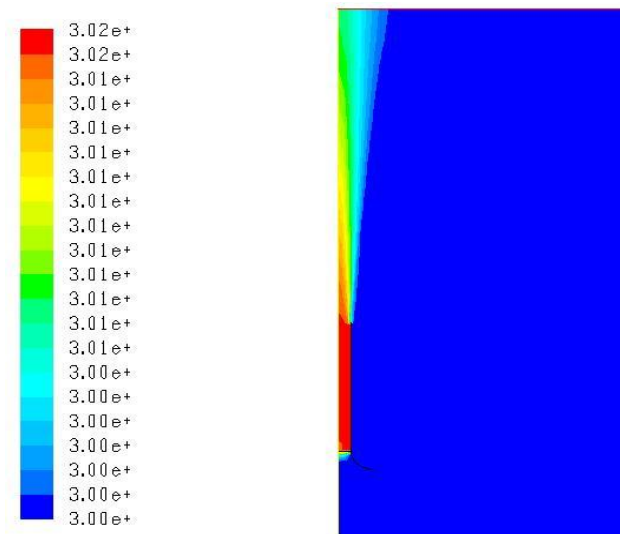
Figur 3-7 Residuals configuration 4

- Configuration 5 converges very well; as one can see in Figur 3-8 Residual configuration 5 Figur 3-8 the residuals are very low after 6000 iterations, only the y-velocity and epsilon residuals are keep the same value (around 10^{-3}).



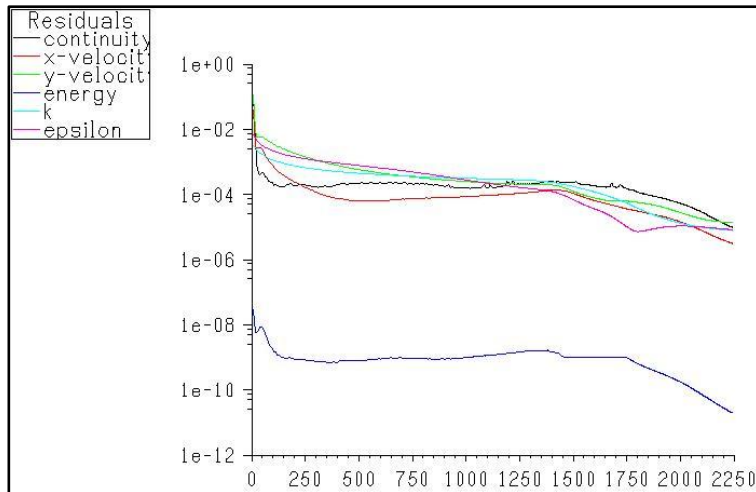
Figur 3-8 Residual configuration 5

The temperatures field (Figur 3-9) is what one might expect, i.e. the inlet temperature is the same as the external and the only differences of temperature appears inside the chimney and in the jet.



Figur 3-9 Temperatures configuration 5

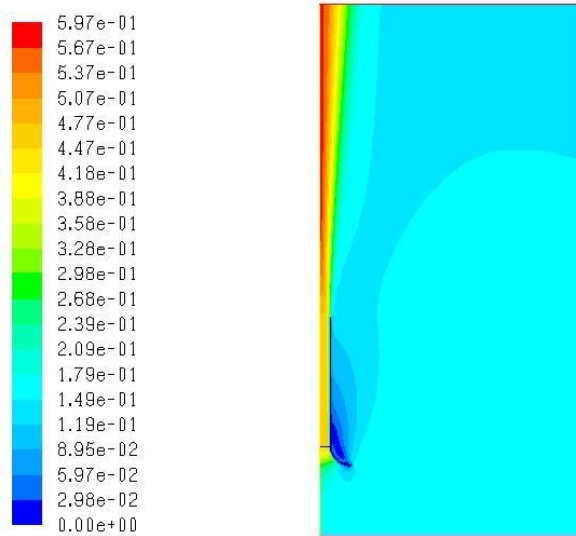
- The Fluent's manual suggests use this configuration in buoyancy effect problems [15]. The value of gauge total pressure was taken following the advice of Fluent's manual.



Figur 3-10 Residuals configuration 6

This configuration is which one gives the best results of convergence. In 2250 iterations, all the residuals are below 10^{-5} , which is taken into account as the value of convergence. The temperatures field is the same as the configuration 6.

The problem of this configuration is the velocity, as one can see in Figur 3-11, the inlet velocity is constant in the whole pressure inlet boundary condition and also the magnitude is close to the velocity inside the chimney. That means, that the influence of the radiation in the value of the flow rate will be minimized due to that the velocity in the inlet boundary condition is around 20% the velocity inside the chimney.



Figur 3-11 Velocity configuration 6

Finally the configuration 5 has been selected due to it is which gives the best relation between convergence and approximation to the real problem in the results (velocity and temperature).

3.2.2 Chimney CFD model

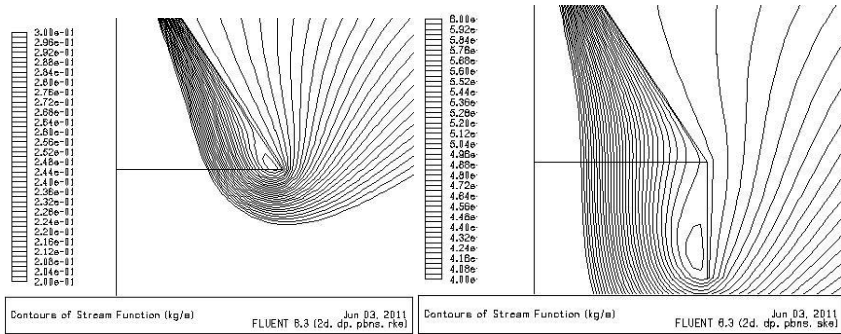
Before making the full model of the chimney, different inlets have been simulated. This action has been made to avoid the recirculation flow that appears in the inlet.

First, the solar collector had been replaced for a radiator boundary condition, fixing the heat flow, to study the flow around the chimney

In the first case (without inlet), one can see the recirculation flow at the inlet, that is the reason why different inlets configurations have been tested to try to avoid this reflow. In any case, these configurations do not affect to the stack effect, as this ones are always before the collector.

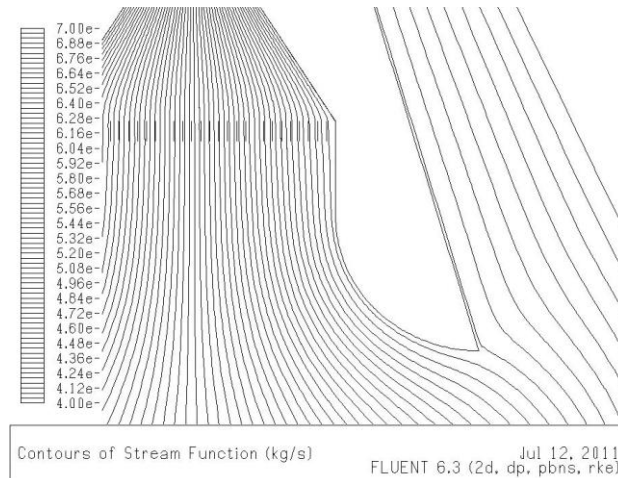
The reason, to find an inlet for the chimney, is that this one will join to a ventilation duct and this reflow hardly appears. Other reasons are the stability of the simulation and the energy balance in the chimney (some of the heat goes out and affect to the stack effect).

The following pictures show the steps to achieve the inlet for the chimney



Figur 3-12 Stream function inlet

Finally, it has been selected the next inlet.



Figur 3-13 Chimney inlet

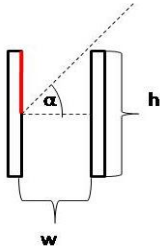
The selected model to simulate the chimney has:

- The boundary conditions selected before.
- The inlet selected, without slip conditions.
- The outside of the chimney is completely different of the inside; the reason is to avoid the reflow what appears on the outside of the inlet.
- The solar collector has been changed for 32 fins. One side of the fin will generated a heat flow, simulating the incident radiation; the other side will be adiabatic.
- The inside (wall and glazing) of the chimney has been considered completely insulated. This approximation can be prove easily:

The U-Value for the glazing is 1.2 W/m^2 , the difference of temperature is around 2K and the area of glazing is $0.75\text{m}^2/\text{m}$, so the heat loss will be:

$$Q = U * A * \Delta T = 1,2 * 0,75 * 2 = 1,776\text{W/m}$$

Usually the input power is around 500W/m , which means that the heat loss is less than 1%.



The heat flow generated in the fins has been estimated with the next equation:

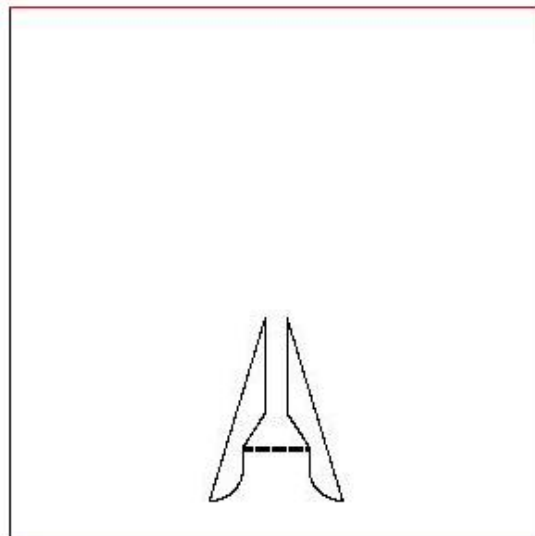
$$\dot{Q} = I \cdot \cos \alpha \cdot \delta \cdot \frac{w}{h} \tan \alpha \quad 3.5$$

$$I = \text{Radiation} \left(\frac{\text{W}}{\text{m}^2} \right)$$

$\alpha = \text{angle between the incident radiation and the horizontal plane}$

$\delta = \text{transmittance of the window}$

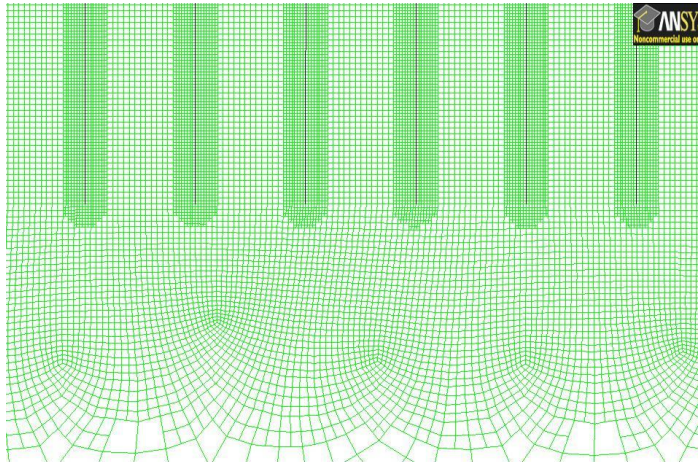
The factor $\frac{w}{h} \tan \alpha$ is the part of the fin which receives the beam radiation (Appendix 2 and Appendix 3).



Figur 3-14 Chimney CFD Model

3.2.3 Grid

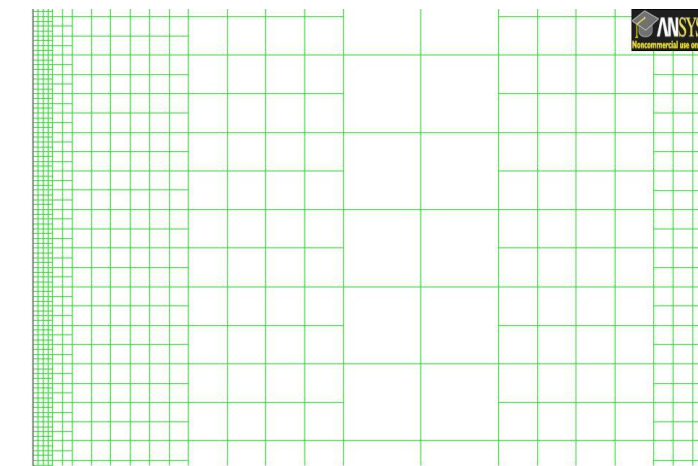
The grid selected has particular care with the velocity and thermal boundary layers in the wall inside the chimney and in the fins of the collector, as one can see in the next pictures.



Mesh

Jun 01, 2011
ANSYS FLUENT 12.1 (2d, dp, pbns, trans-sst)

Figur 3-15 Grid fins



Mesh

Jun 01, 2011
ANSYS FLUENT 12.1 (2d, dp, pbns, trans-sst)

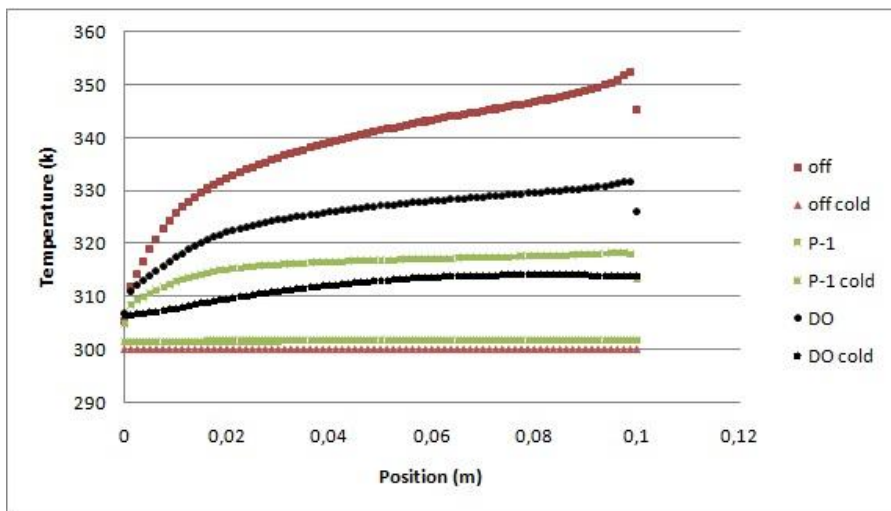
Figur 3-16 Grid wall

3.2.4 Radiation model

Three types of radiation models have been studied to achieve the best approximation of the real problem:

- Non radiation
- DO model
- P-1 Model

Figur 3-17 shows the temperature of the both side of the fin. For the non-radiation the temperature gap between the both side is too high and does not make sense. On the other hand the gap, in the other two models, is almost the same (10°C), but in the P-1 model the temperature is lower around 18°C for the hot side and in the experimental results the increase of temperature is around 25°C.



Figur 3-17 Fin temperature. Different radiation models

DO model has been selected, even it uses most resources and time, is which one more realistic result obtains. Moreover it is the only model, who allows simulates a semitransparent wall what it is going to be important in next sections.

3.2.5 Turbulence model

As the Reynolds and Rayleigh suggest, the problem is a transition-turbulent flow. Therefore, the turbulent models and wall treatment, selected to

compare with the experimental results, have been taken in account this assumption.

Four models of turbulence had been tested; k-e model, Transition k-kl-w model, Transition SST model and Reynolds stress model.

In the k-e model, the lash of full buoyancy effect and thermal effect were ticked due to the flow across the chimney is leaded of these effects. Two near wall treatment has been simulated; the Standard wall function and the Enhanced wall treatment. Also two k-e models were taken in account; the Standard model and the Realizable model.

3.2.5.1 *Setting values*

The difference of the velocity at the outlet of the chimney is insignificant, when the radiation varies between 881.7 W/m² and 846.4 W/m², as the experimental data shows. Therefore, the average of these two radiations (864.05 W/m²) has been selected as an incident radiation of the CFD simulations. Then the heat flux generated on the fins is:

$$\begin{aligned} \dot{Q} &= I \cdot \cos \alpha \cdot \delta \cdot \frac{w}{h} \tan \alpha \\ \dot{Q} &= 864,05 \cdot \cos 33^{\circ} \cdot 0,63 \cdot \frac{0,044}{0,07} \tan 33^{\circ} = 186,35 \text{ W/m}^2 \end{aligned} \quad 3.6$$

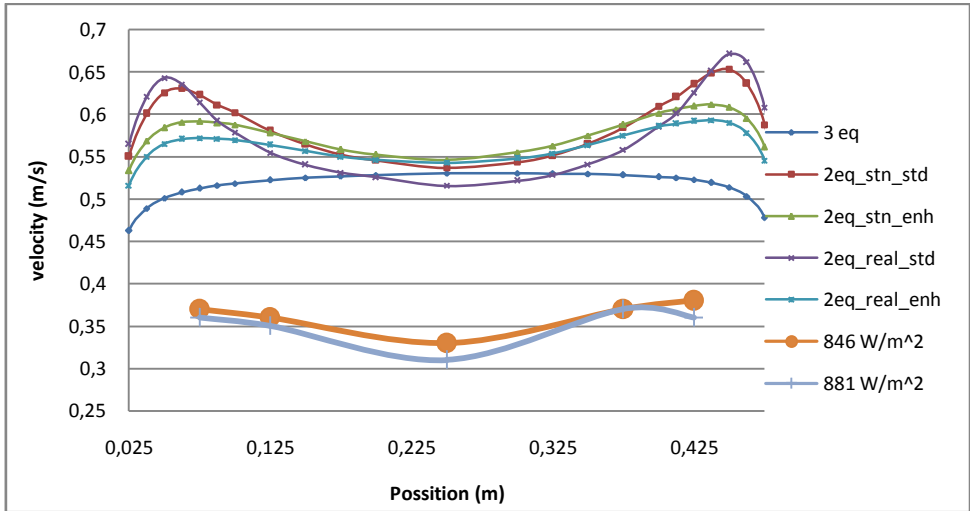
3.2.5.2 *First simulation*

In the first simulations, the turbulence values of the boundary conditions (k and e) and the turbulent model constants are the default.

In this case the transition SST model (4 equations) and the Reynolds stress model (5 equations) had problems with the convergence, so these models were discarded for next simulations.

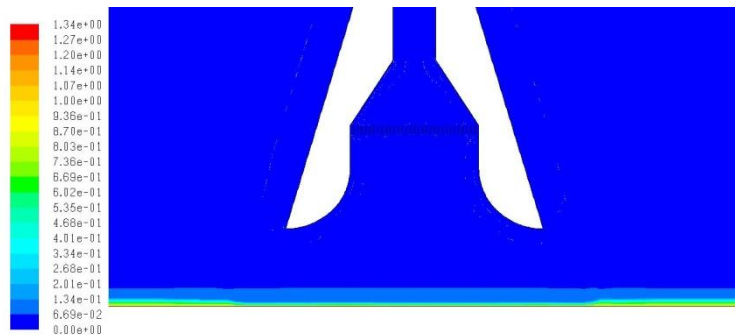
Figur 3-18 shows the velocity profiles in the outlet velocity for the turbulence models and the experimental results of a 3 m high chimney. In all the cases the velocity is almost the double of the experimental. Before changed the values of the turbulent model constants and boundary condition, some model has been removed:

- The Transition k-kl-w model has removed because the velocity profile is uniform and the experimental results shows that closed to the wall the velocity is higher than in the center.
- The k-e model with Standard wall functions owing to the opposite, the difference of velocities is too higher compare to the experimental results.



Figur 3-18 Velocity profile in the outlet (first simulation)

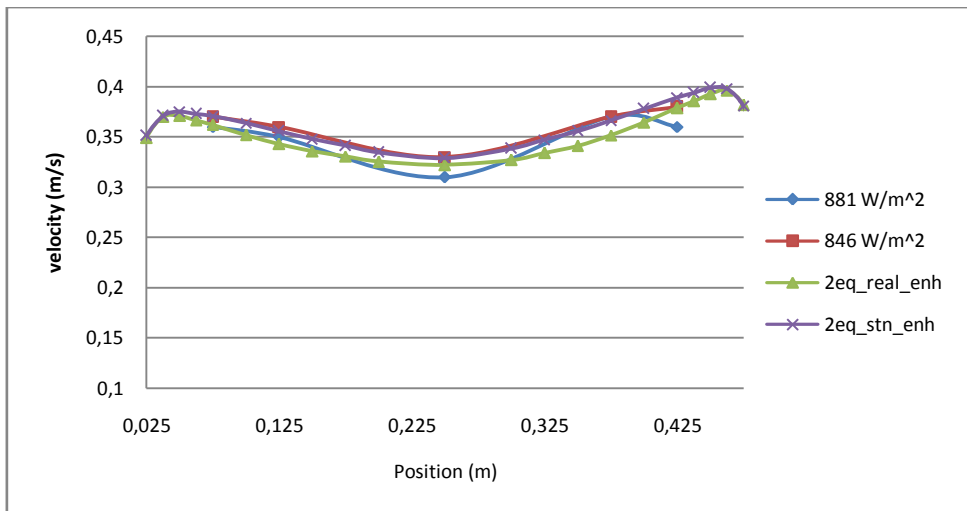
It had been compared the graphics of turbulence properties of the flow, to know what changes have to make in the turbulence models. Figur 3-19 shows the contours of turbulent dissipation rate (ϵ) and the mistake of the model, as one can see the value of ϵ is too high in the pressure outlet and velocity inlet boundaries conditions.



Figur 3-19 Profiles of turbulent dissipation rate

3.2.5.3 Second simulation

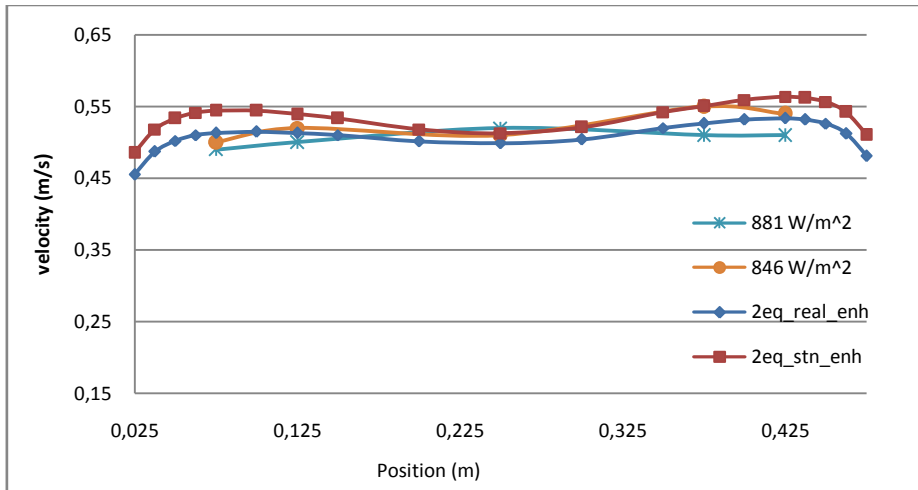
Changing the turbulent dissipation rate (ϵ) to 0.3 in the velocity inlet and pressure outlet boundary conditions, the CFD results agree with the experimental as it is shown in Fig. 3-20. The difference between the Standard k- ϵ model and Realizable k- ϵ model is that the velocity in the last one is a little bit lower.



Figur 3-20 Velocity profiles h=3m

For height of the chimney of 4.15m (Fig. 3-21) the velocity profiles of experimental and CFD simulations are also similar.

To select the turbulence model, it has been compared the average velocity of the experimental results and the CFD simulation for both heights (Table 3). For 3m the two turbulent models are inside the limits forced for the experimental velocities, but for 4.15m the Standard k- ϵ is upper this limits. Therefore the Realizable k- ϵ model with Enhanced wall function was chosen to simulate the solar chimney.



Figur 3-21 Velocity profiles h=4,15m

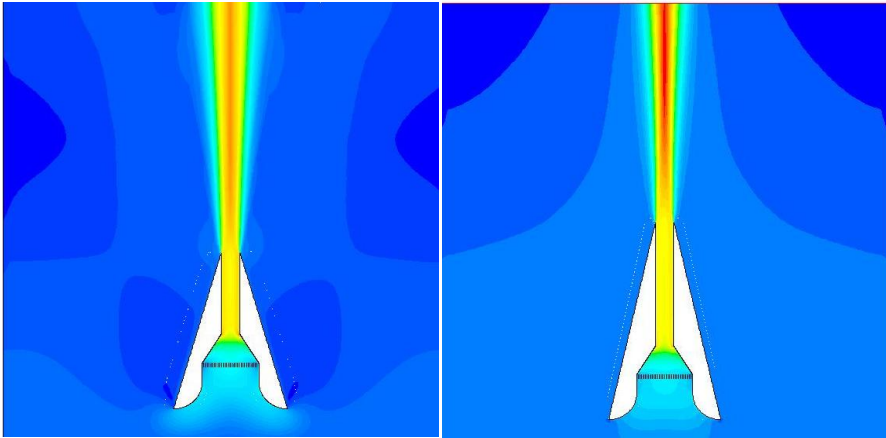
Radiation (W/m ²)	Velocity h=3m (m/s)	Velocity h=4,15m (m/s)
881,7	0,350	0,506
846,4	0,362	0,524
2eq_real_enh	0,350	0,515
2eq_stn_enh	0,361	0,539

Table 3 Comparison of velocity. Experimental Vs CFD

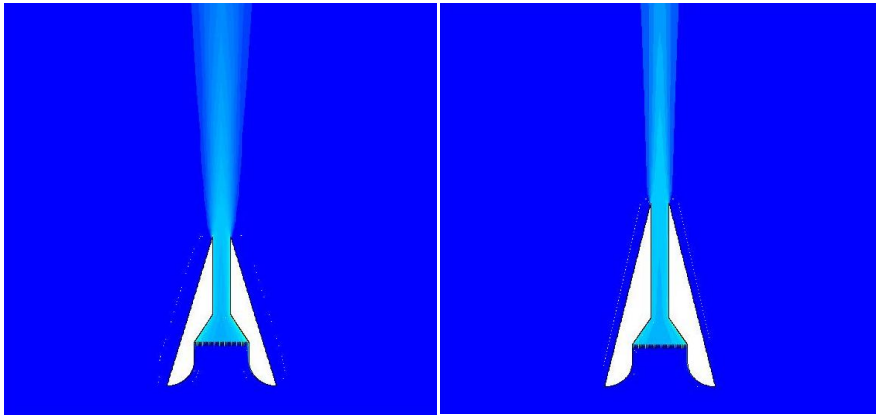
3.2.6 Results

As a summary the CFD model selected to simulate the solar chimney and which one gives the more realistic results is:

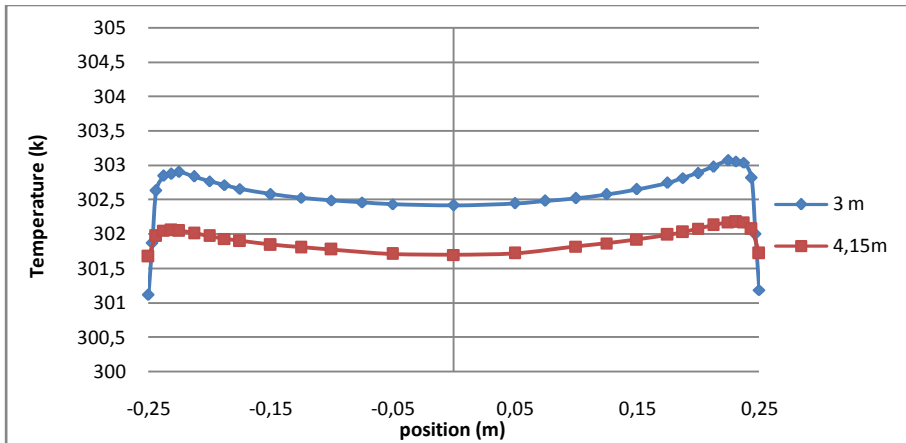
- The boundary conditions are a velocity inlet in the bottom of 0.01 m/s with a inlet temperature of 300 K, the inlet turbulent kinetic energy of $1 \text{ m}^2/\text{s}^2$ and a turbulent dissipation rate of $0.3 \text{ m}^2/\text{s}^3$; the right and the left side is a wall with slip condition and a temperature of 300 K; and the top is a pressure outlet with the same backflow conditions as the velocity inlet. Appendix 4
- A smooth chimney inlet to avoid the recirculation.
- The radiation model is DO model with 4 theta and pi divisions, 4 theta and pi pixels and 10 flow iterations per radiation iteration.
- The Realizable k-e model with Enhanced wall function.



Figur 3-22 velocity contours 3m and 4,15m



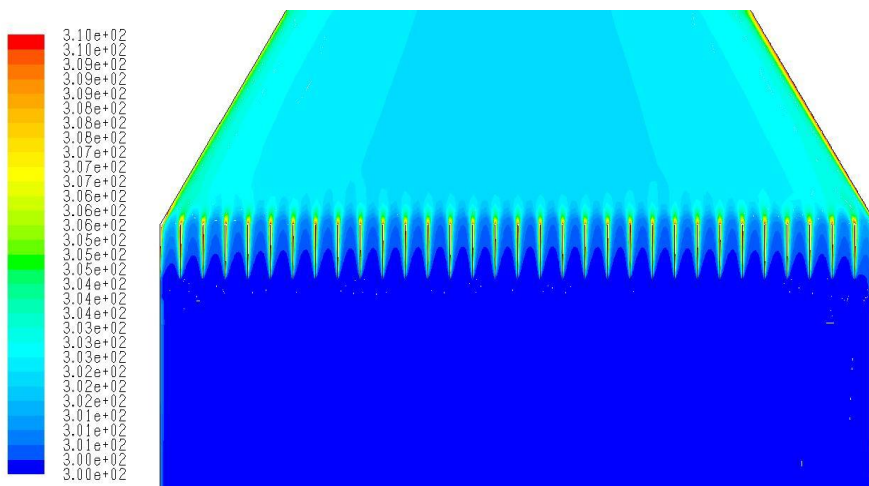
Figur 3-23 Temperature contours 3m and 4,15m



Figur 3-24 Temperatures profiles in chimney outlet

The before figures show an interesting conclusions

- The flow across the model can be considered as a symmetric (Figur 3-22)
- The temperature is almost constant inside the chimney (Figur 3-23, Figur 3-24 and Figur 3-25)
- The whole height of the chimney is taking into account in the stack effect. This is the main difference on the other types of solar chimneys.

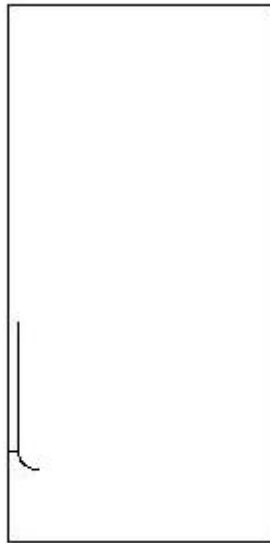


Figur 3-25 Temperature contour of the collector

3.3 Simplification of the model

As one can see on the before results, the flow inside the chimney can be consider as symmetric and with constant temperature. This fact suggests change the model to a symmetric one with a coarse grid to future simulations of the chimney.

The proposed model has the same turbulent model, radiation model, boundary conditions (except for the symmetry) and the inlet. On the other hand, the chimney's width is constant and equal to the outside of the chimney (0.5 m); the solar collector has been replaced to a radiator boundary condition; and the use of the radiation model will be study.



Figur 3-26 Simplified model

3.3.1 Setting

The model has to have the same power as the real one, which means that the heat flux in the radiator and the collector is not the same. The ratio between the heat fluxes is the next:

$$\begin{aligned}
 P &= I_{real} \cdot A_{collector} = I_{radiator} \cdot A_{radiator} \\
 I_{radiator} &= I_{real} \frac{A_{Collector}}{A_{radiator}} = I_{real} \frac{\text{number of fins} \cdot h_{fin}}{A_{radiator}} \\
 I_{radiator} &= I_{real} \frac{33 \cdot 0,07m^2}{0.5m^2}
 \end{aligned}$$

$$I_{radiator} = 4,62 \cdot I_{real} \quad \mathbf{3.7}$$

If there is not any setting in the model (except for the heat flux), it is easy to check that the flow rate and the temperature will be higher. Therefore is necessary to introduce a pressure drop in the radiator.

Following the advices of Fluent's Manual [15], it has been calculated the difference of the coefficient of pressure drop between the real and the simplification model for three heat powers in the radiator. Table 4 shows that the difference is approximately constant, and one can assume that the pressure drop across the radiator is the average of this values, what is $K=0.5$

Q (W)	Difference K
150	0,467630484
450	0,528222212
960	0,498409162

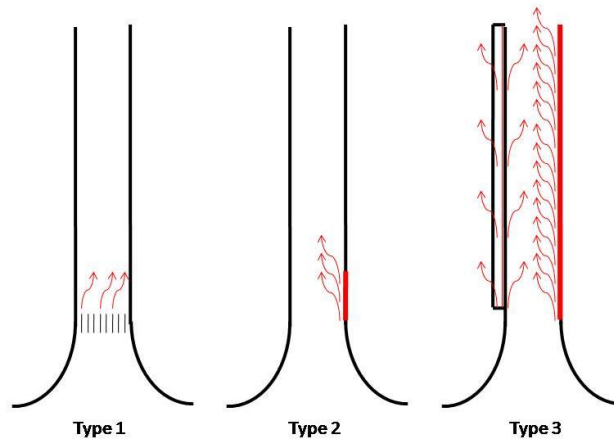
Table 4 Difference Coefficient of pressure drop

Also, this value can be calculated easily, assuming the difference of pressure drops, between the real and the simple model, is the reduction between the inlet and the outlet. The pressure drop coefficient of a nozzle is usually constant and can be estimate in tables; in this case the value is around $K=0.48$.

3.4 Comparison different solar chimneys types

The two models studied in this section has the same geometry, also the same boundary condition, turbulent and radiation models and the same assumption of the solar radiation can be estimated as a heat flux in the wall.

The solar radiation (I_{sun}) is the same in all the models to compare the difference of these three solar chimneys



Figur 3-27 Models of the types of solar chimney

- **Type 1**

This model is the simplification of the solar chimney in the EPT-lab. The heat flux in the radiator has the following equation

$$\dot{Q} = I_{sun} \cdot 4,62 \cdot \cos \alpha \cdot \delta \cdot \frac{w}{h} \tan \alpha \quad 3.8$$

- **Type 2**

This is the model of the Swedish school. The solar collector (absorption wall) has always the same height (0,5 m) and the heat flux generated is:

$$\dot{Q} = I_{sun} \cdot \cos \alpha \cdot \delta \quad 3.9$$

As the equal as the model type 1, it has been assumed that the walls of the chimney are completely insulated and there is no appreciable effect of the window in the solution of the simulation.

- **Type 3**

This is the standard solar chimney for mild climates, the southern wall is a glazing and the interior northern wall is the solar collector. In this case, the assumption of insulated wall is not possible in the

glazing. Therefore, a new boundary condition for the glazing had developed:

The characteristic of the glazing (Appendix 2) shows that a percentage of the solar energy is transmitted (63%), other is reflected (23%) and other is absorbed (14%). This absorbed radiation is simulated as a heat generation rate (W/m^3) inside the window:

$$Q_{glazing} = \frac{\gamma \cdot I_{sun} \cdot \cos \alpha}{e} \quad 3.10$$

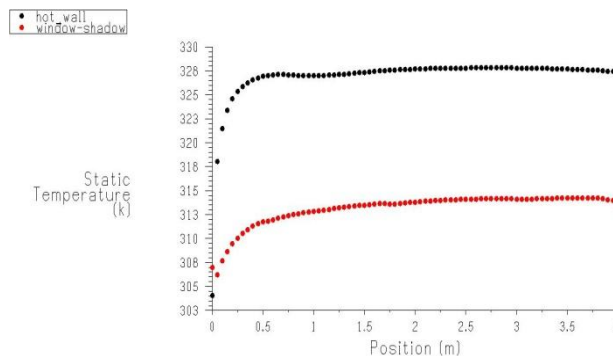
γ = percentage of solar absorption
 e = thickness of the glazing

Furthermore, the glazing properties (density, conductivity, absorption coefficient, c_p) has been put in the boundary conditions of the southern wall.

The heat flux in the solar collector is the same as the type 2, equation 3.9

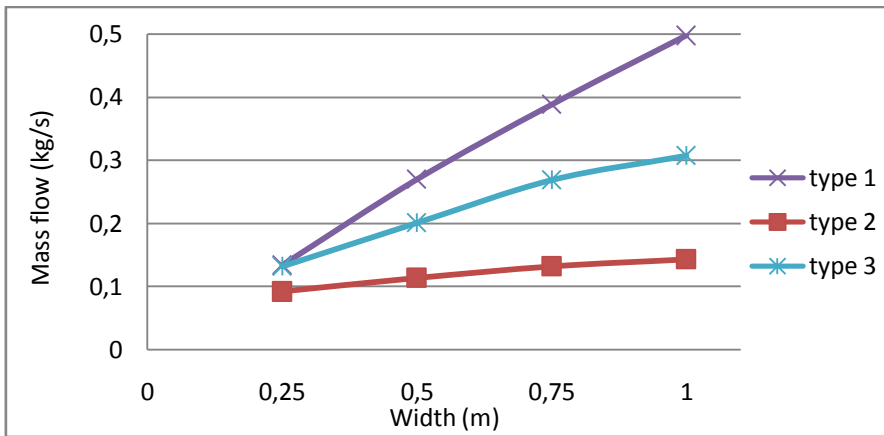
3.4.1 Results

The results of the temperature in the solar collector and the glazing have been compared with the simulations carried out in other work [7], that show an increment around 30°C in the solar collector and 12°C in the glazing, which is similar to the results simulated, 28°C and 13°C correspondingly (see Figur 3-28).



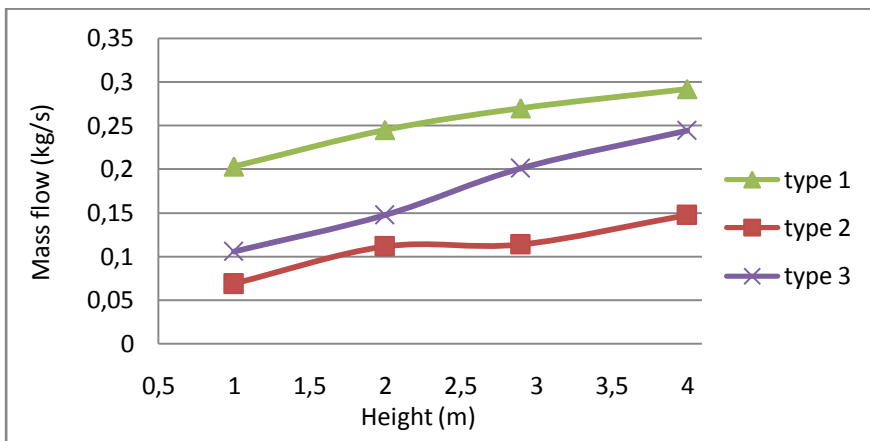
Figur 3-28 Temperatures in type 3

The comparison was carried out with 8 simulations for each chimney, 4 different widths ($h=3\text{m}$) and 4 heights ($w=0.5\text{m}$).



Figur 3-29 Mass flow Vs Width

Figur 3-29 shows the chimney type 1 has a linear mass flow increase with the width; the reason is the area of solar collector increase. Note, if the width is small ($w<0.25\text{m}$) the flow rate of the chimney type 1 will be lower than the other chimneys; that is one of the reasons of this kind of chimneys (type 2 and 3) has usually a width around 0.25 m [1, 2, 7].



Figur 3-30 Mass flow Vs Height

On the other hand, if the height increases the flow rates enhance, but in this case the chimney type 3 increases the area of solar with the height and therefore, the slope of the flow is higher (Figur 3-30), which means that

chimney type 3 gets higher flow when the height of the chimney is enough high, in this case around 5 m. Note that, the slop changes between 2 m and 3 m in the chimneys type 2 and 3, the reason is the link of the two thermal layers (southern and northern walls).

3.5 Performance of the solar chimney

3.5.1 Theoretical equation

Taking into account a uniform velocity and temperature inside the chimney, as it was demonstrated in 3.2.6, the theoretical flow rate will be:

- Energy balance in the chimney

$$\begin{aligned} Q &= q\rho c_p(T_{out} - T_{ext}) \\ T_{out} &= T_{ext} + \frac{Q}{q\rho c_p} \end{aligned} \quad 3.11$$

- Approximation velocity profile constant

$$V \cdot A = q \quad 3.12$$

- Drag coefficient Vs constant pressure loss

$$Cd = \frac{1}{\sqrt{\sum K_{loss}}} \quad 3.13$$

- Bernoulli equation

$$\begin{aligned} \rho gH \frac{(T_{out} - T_{ext})}{T_{ext}} &= \frac{1}{2} \rho V^2 \sum K_{loss} \\ \rho gH(T_{out} - T_{ext}) &= \frac{1}{2} \rho T_{out} \left(\frac{q}{ACd} \right)^2 \\ q^3 + q^2 \frac{Q}{T_{ext} \rho c_p} - \frac{(ACd)^2 2gHQ}{T_{ext} \rho c_p} &= 0 \end{aligned} \quad 3.14$$

The value of C_d can be calculated as a function of the sum of coefficient of pressure loss of the inlet, the nozzle, the outlet and the friction of the walls

$$\sum K = K_{inlet} + K_{nozz} + K_{outlet} + f \frac{H}{Dh} \quad 3.15$$

In the Appendix 1, one can find the values of this coefficient depending the geometry

In theory, C_d is function of the flow rate, because the factor f depends of the number of Re , but $f \in (0.04, 0.015)$ which gives a $Cd \in (0.75, 0.788)$, who is not a big difference. Therefore one can consider the Cd as function only of the height:

$$\sum K = 0.04 + 0.48 + 1 + 0.04 \frac{H}{0.5}$$

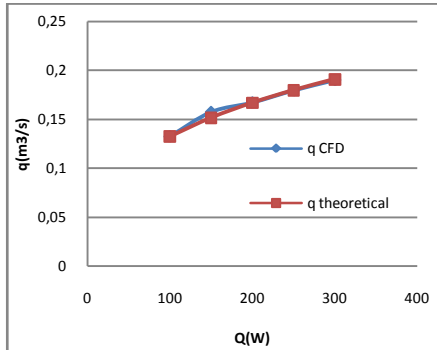
$$Cd = \frac{1}{\sqrt{1.52 + 0.08H}} \quad 3.16$$

The solution of equation 3.14 is longer to show, but the method to resolve a third degree equation can be found in [13]

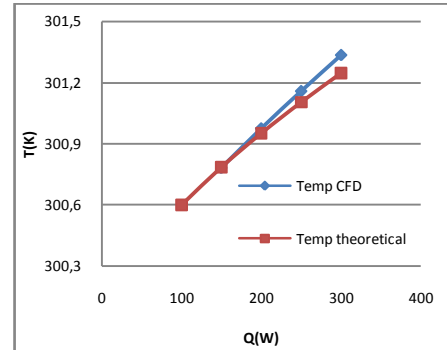
3.5.2 Validation of the theoretical equation

To valid the equation 3.14, 9 simulations have calculated; 5 for diverse values of Q (100 W to 300W) and 4 for diverse values of height (1m to 4m). The reference value of Q is 300 W, of H is 3m, except the cases when varies one of this values.

3.5.2.1 Flow rate as a function of radiation

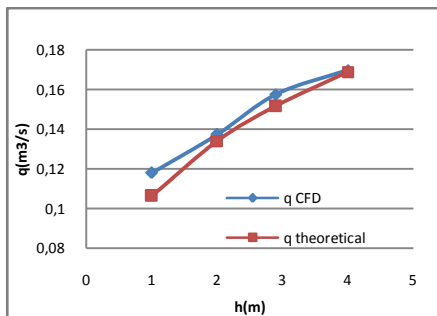


Figur 3-31 q Vs Q (H=cte)

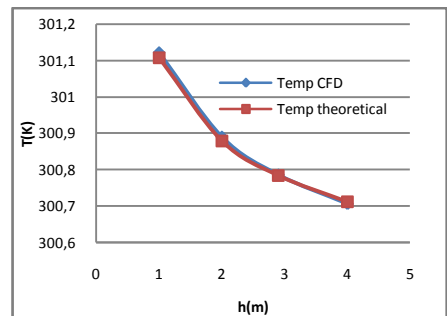


Figur 3-32 Temperature Vs Q (H=cte)

3.5.2.2 Flow rate as a function of height



Figur 3-33 q Vs H (Q=cte)



Figur 3-34 Temperature Vs H (Q=cte)

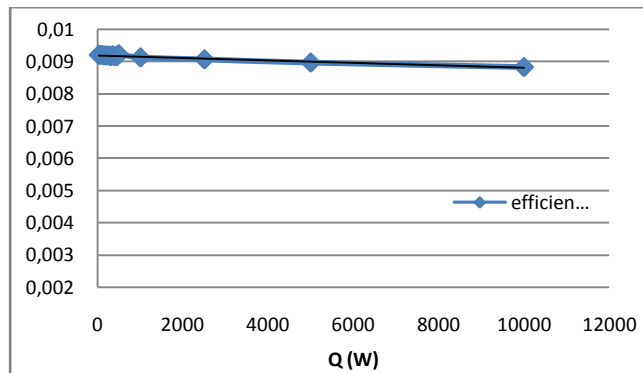
As one can see in the results, the theoretical equation estimates with precision the values of flow rate and temperature in the chimney.

The kinetic energy efficiency is one of the solar chimney properties allows compare with other technologies. This efficiency can be calculated as the coefficient between the kinetic energy and the power generated in the solar collector:

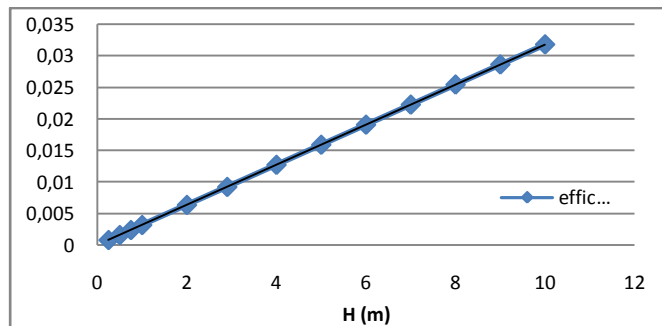
$$\eta = \frac{\frac{1}{2}mV^2}{Q} = \frac{\frac{1}{2}q\rho\left(\frac{q}{A}\right)^2}{Q}$$

$$\eta = \frac{q^3\rho}{2QA^2}$$

3.17



Figur 3-35 Efficiency (%) Vs Q



Figur 3-36 Efficiency (%) Vs H

Figur 3-35 and Figur 3-36 show that if one wants to improve the efficiency of the solar chimney, he has to increase the height of the chimney and not the area of the solar collector (more heat generation).

Another important conclusion of both figures is that the efficiency is constant with the radiation (Q) and increase linearly with the height, which means:

$$q = \sqrt[3]{\frac{\eta 2QA^2}{\rho}} \quad \text{and} \quad q = \sqrt[3]{\frac{cteH 2QA^2}{\rho}}$$

The value of this constant or η can be calculated if the Boussinesq approximation is supposed for a gas

$$\frac{\Delta T}{T} = \beta \Delta T \quad 3.18$$

Thus the new equation for the flow rate will be:

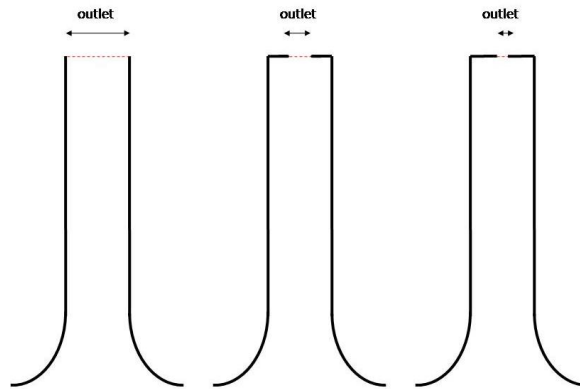
$$\begin{aligned} gH\beta(T_{out} - T_{ext}) &= \frac{1}{2} \left(\frac{q}{ACd} \right)^2 \\ \rho H\beta \frac{Q}{q\rho c_p} &= \frac{1}{2} \left(\frac{q}{ACd} \right)^2 \\ q &= \sqrt[3]{\frac{(ACd)^2 2gH\beta Q}{\rho c_p}} \end{aligned} \quad 3.19$$

Also, this demonstrates, as a good election, the supposition of Boussinesq for the CFD simulations.

3.5.3 Pressure Vs Flow rate

The function Pressure Drop Vs Flow rate serves to know the behavior of the chimney for different pressures loss and also to compare with fans, since the cross between these curves (system and fan) marks the operations point.

A simple control valve was designed to simulate diverse conditions of work, this valve consist in two plates, situated in the outlet, are closing form the outside in (see Figur 3-37).



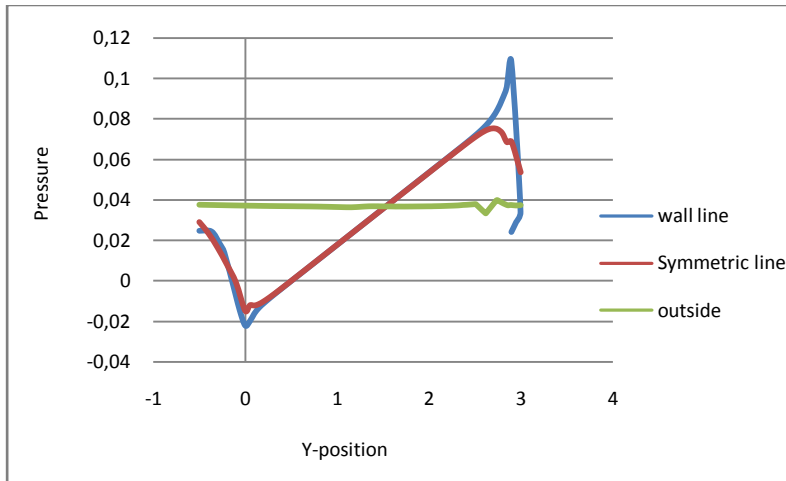
Figur 3-37 Behavior of the control valve

Six simulations were carried out for diverse openings of the valve, from fully open to 10% of aperture. Less percentage of opening makes the simulation unstable and also the assumptions of adiabatic wall does not satisfy because the increase of the air temperature.

To calculate the pressure drop across the chimney, it has been taken the pressure data from 3 lines: one is the symmetric line, other pass close to the wall (0.05m from the wall) and the other is parallel to these ones and outside from the chimney.

The outside line serves to calculate the hydrostatic pressure (equation 3.20), since Fluent uses a reduction constant (A) for the simulations. Once the hydrostatic pressure is calculated, this value is related to data from the chimney's lines. Figur 3-38 shows these values from 80% of valve aperture; except in the inlet and the outlet the two lines follow a straight line which is calculated to know the average pressure drop across the chimney.

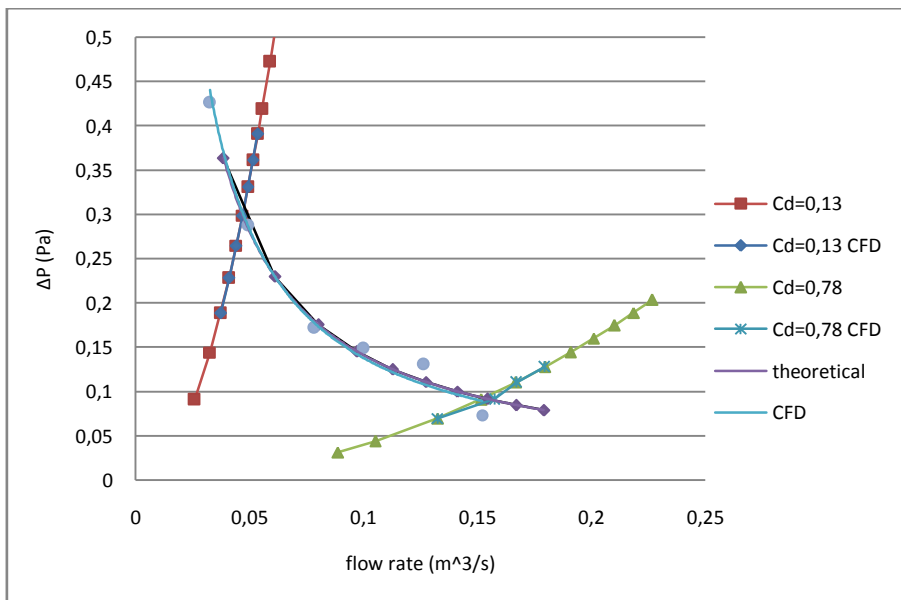
$$\Delta P_H = A \rho g \Delta H \quad 3.20$$



Figur 3-38 Hydrostatic pressure from the chimney

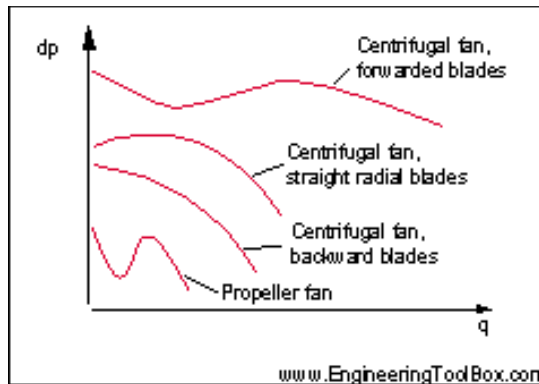
Furthermore, it was carried out simulations for diverse incident radiation (Q) from both, fully and 20% opening, as a comparison of system curve.

The results of these simulations and the theoretical results from equation 3.14 are shown in Figur 3-39. As one can see, there are several differences between a chimney curve and a fan curve (see Figur 3-40):



Figur 3-39 Pressure Vs Flow rate

1. There is not a maximum or minimum, which means that the slope is always negative and therefore the operation point is always stable.
2. Meanwhile there is a lower limit for stall in the fans, the chimney always can generated a flow rate no matter how small it is.
3. The disadvantage is the strong dependence between the flow rate and the pressure in the chimney, when the desirable is to have the same pressure drop.

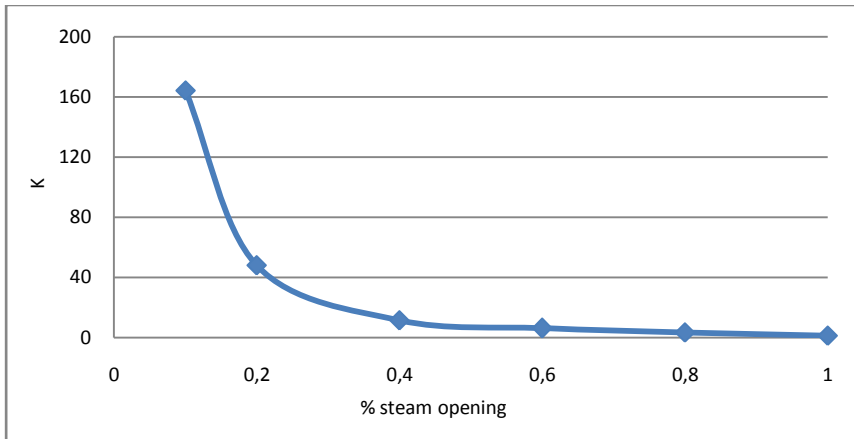


Figur 3-40 Curves of different types of fan

3.5.4 Study of the control valve

This purpose of this section is study the viability of the valve control design previously (Figur 3-37).

First, it has been calculated the coefficient of pressure loss in function of the % opening (Figur 3-41). The result shows a higher increase of the coefficient with an opening less than 40%.



Figur 3-41 K Vs % opening

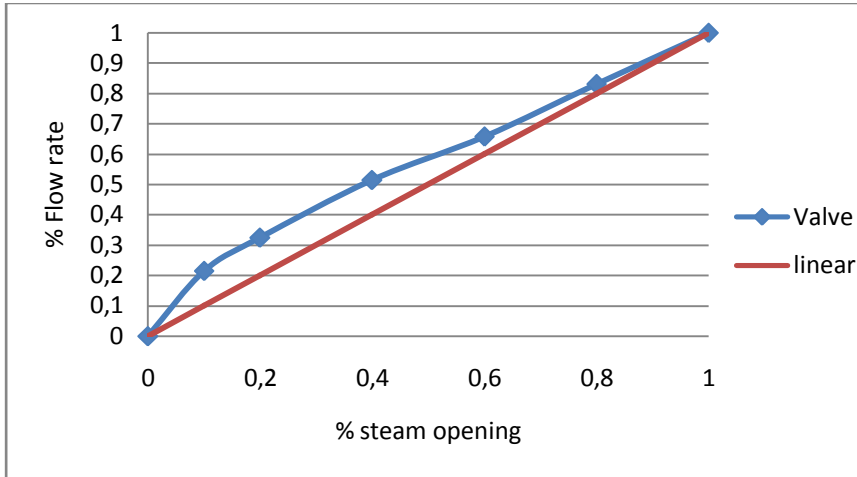
Figur 3-42 shows % of flow rate Vs % of opening for the system (chimney + valve). Ideally, a valve control should have a linear curve, which means that if it has a 50% of opening, the flow rate will be 50%. In this case the curve is between a linear curve and a quick opening curve (see Figur 3-43). Usually it is suggested to choose a quick opening valve for open/close system and not for control.

Also, it is interesting to know the authority of the valve:

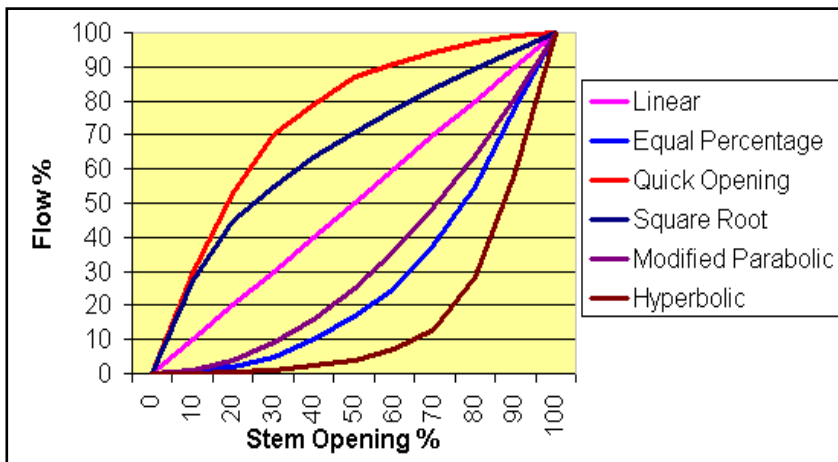
$$A = \frac{\Delta P_{valve} (100\%)}{\Delta P_{system}} = \frac{K_{valve} (100\%)}{\sum K_{system}}$$

$$A = \frac{1}{1.52 + 0.08H} \quad \mathbf{3.21}$$

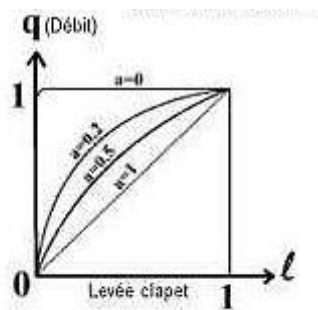
For this case ($H=3m$), $A=0.57$, the progressiveness of the system is not the best but it is closed, but if the pressure loss of the system increase, means that the authority decrease and the system approach to a quick opening valve (see Figur 3-44). Even though the design is simple and cheap to carry out, the facts suggest choose another valve with a flow characteristic as the hyperbolic or modify hyperbolic types.



Figur 3-42 % flow rate Vs % opening



Figur 3-43 Control valve flow characteristics

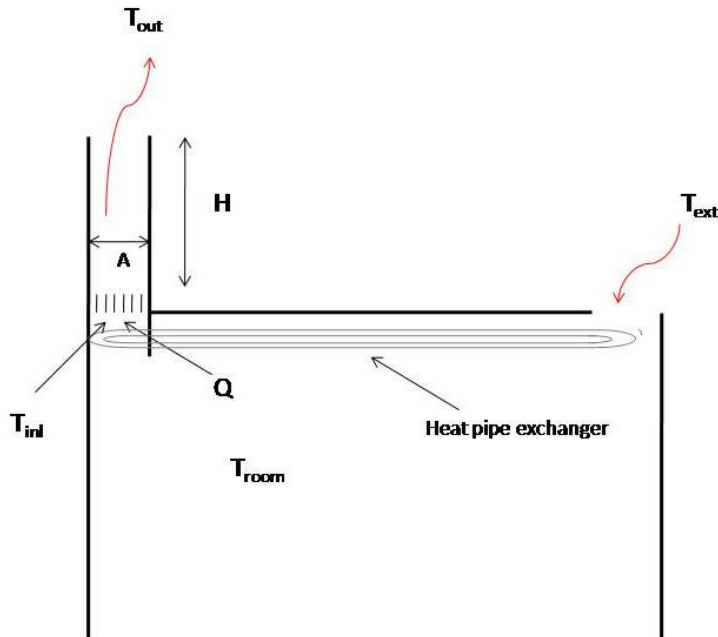


Figur 3-44 Effect of authority in a linear valve

4 Behavior of a building with a solar chimney

This section pretends to achieve a theoretical equation for solar chimney attached to a house and simulate diverse conditions studying the effect of the solar chimney in the flow rate.

4.1 House model



Figur 4-1 House model

- Efficiency of the heat recovery

$$\varepsilon = \frac{T_{inl} - T_{room}}{T_{ext} - T_{room}}$$

$$T_{inl} = \varepsilon(T_{ext} - T_{room}) + T_{room} \quad 4.1$$

- Energy balance in the chimney

$$Q = q\rho c_p(T_{out} - T_{inl})$$

$$T_{out} = \frac{Q}{\rho q c_p} + \varepsilon(T_{ext} - T_{room}) + T_{room} \quad 4.2$$

- Boussinesq approximation: Equation 3.18

- Approximation velocity profile constant: Equation 3.12
- Drag coefficient Vs constant pressure loss: Equation 3.13
- Bernoulli equation

$$\begin{aligned} \rho g H \beta (T_{out} - T_{ext}) + \Delta P_{fan}(q) + \frac{1}{2} \rho C_p V_{wind}^2 &= \frac{1}{2} \rho V^2 \sum K_{loss} \\ \rho g H \beta \left(\frac{Q}{\rho q c_p} + (\varepsilon - 1)(T_{ext} - T_{room}) \right) + \Delta P_{fan}(q) + \frac{1}{2} \rho C_p V_{wind}^2 &= \frac{1}{2} \rho \left(\frac{q}{A} \right)^2 \sum K_{loss} \\ g H \beta \frac{Q}{c_p} + q \left[(\varepsilon - 1)(T_{ext} - T_{room}) \rho g H \beta + \Delta P_{fan}(q) + \frac{1}{2} \rho C_p V_{wind}^2 \right] &= \frac{1}{2} \rho \frac{q^3}{A^2} \sum K_{loss} \\ q^3 - q (A C d)^2 \left[(\varepsilon - 1)(T_{ext} - T_{room}) 2 g H \beta + \frac{\Delta P_{fan}(q)}{2 \rho} + C_p V_{wind}^2 \right] - 2 (A C d)^2 g H \beta \frac{Q}{\rho c_p} &= 0 \end{aligned} \quad 4.3$$

This is a third degree equation and can be resolve, but the solution is long and depends of the fan. The method to solve this equation can be found in [13].

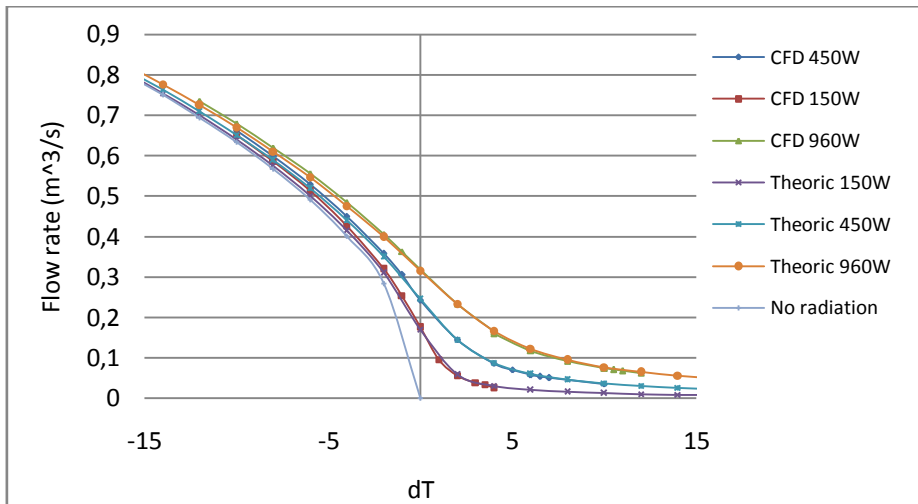
4.2 Effect of difference of temperatures

This case studies the effect of a Temperature in the room (i.e. inlet temperature in the chimney) different from the external temperature. Which means that the only variable parameters are Q (radiation) and the difference of temperatures, fixing the others (Cd, A, H...). It is been considered that is natural ventilation (no fan and heat recovery) and also there is not wind effect.

First, it has been compared the theoretical equation of flow rate with CFD simulations. The CFD model is the same as the other times except that before the radiator (0,1m) there is a new boundary condition; a new radiator which gives a jump of temperatures, thus the inlet temperature can be fixed easily.

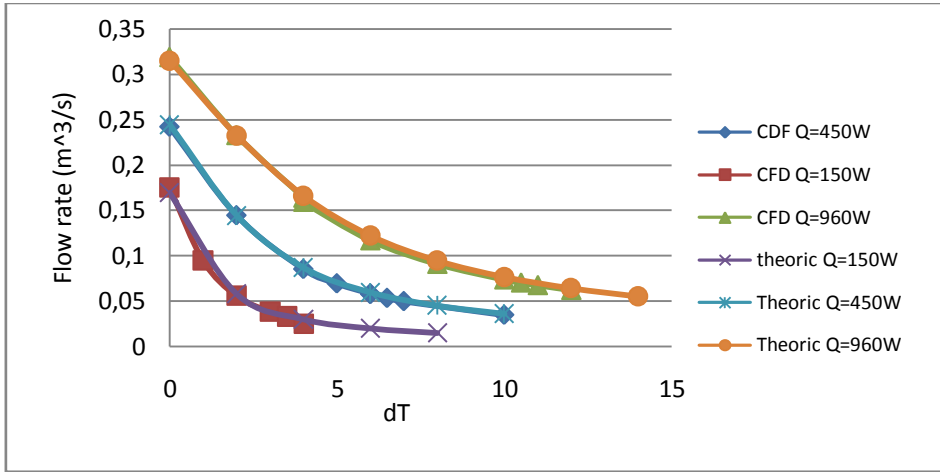
Three different radiation have been simulated (150, 450, 960 W), with a difference of temperatures ranging from -10 to 12 degrees. Have been noted that when the flow rate is very low (less than 0.1m³/s) the simulation start to be unstable, and until this, if the difference of temperature increase (depending the input power), the flow rate is negative (the flow change the direction), therefore the theoretical equation 4.3 is not satisfied.

Figur 4-2 and Figur 4-3 shows that the CFD results and the theoretical are very similar, therefore, from here, it is not necessary to do more simulations, and the results from the equation 4.3 will be considered valid. Only in the cases with a flow rate less than $0.05\text{m}^3/\text{s}$ the equation 4.3 does not work, because the assumptions of turbulent flow and Boussinesq fluid do not satisfy.



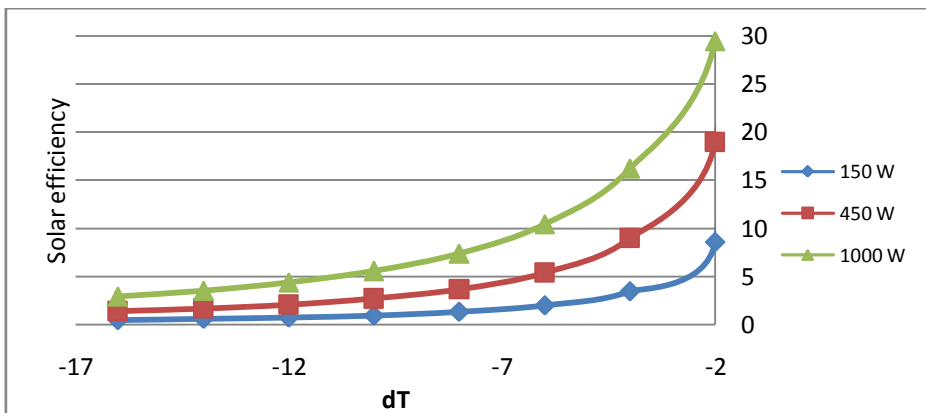
Figur 4-2 Flow rate Vs difference of temperatures

The first conclusion that one can obtain for the results is the strong relation between the difference of temperatures (dT) and the flow rate. When dT decrease ($T_{\text{room}} \gg T_{\text{ext}}$) increase the flow rate, and the effect of solar assistance (radiation) decrease, this effect is shown in Figur 4-4. Obviously the solar efficiency depends of the solar radiation, it is one of the conclusion of Cito Alfonso 2000 [1]; but it also depends of dT and the effect of solar radiance can be neglect with a $dT < -12$ °C. On the other hand, if dT is enough high (>10 °C), the flow rate will be zero and the solar radiation does not have enough power to generate an efficient flow rate. Therefore the effect of a solar chimney compared with a normal chimney only takes into account around $-12 < dT < 10$ °C. This conclusion is estimated and it depends on the height and the solar radiation.



Figur 4-3 Flow rate Vs dT>0

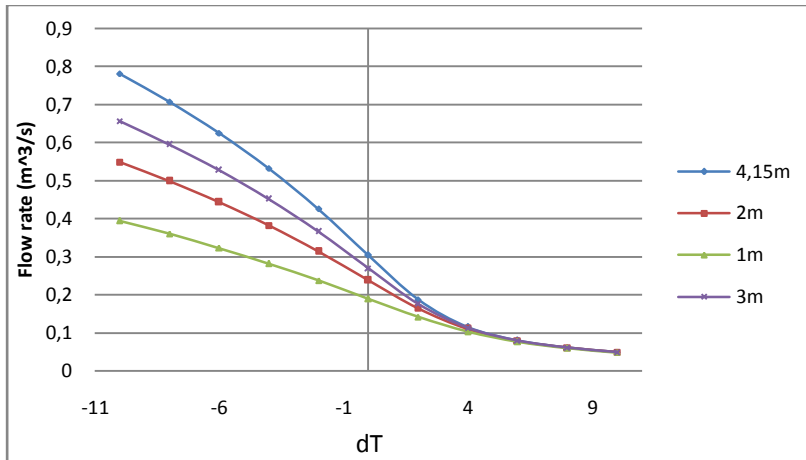
Figur 4-3 shows the behavior of the house model if the $T_{\text{room}} < T_{\text{ext}}$. There is no difference appreciable between the results of CFD-model and the theoretical equation, even in the cases when the CFD simulations were problems with the convergence (the last point), this evince the good approximation of the equation 4.3. Also there is a significant difference of the flow rate with diverse values of solar radiation.



Figur 4-4 Solar efficiency Vs difference of temperature

4.3 Effect of the height of the chimney

This section tries to show the behavior of the solar chimney with various height and temperatures. The value of the solar radiation is fixed (600W) and the other variables the same.



Figur 4-5 Flow rate vs. dT (various height)

As one can expect (Figur 4-5), if the temperature in the room is higher than the surroundings, the behavior of the solar chimney is similar to a normal one i.e. more height means more flow rate. However, if the temperature in the room is lower than the surroundings (Figur 4-5) from 4°C, there is no difference between diverse heights. That is an important result because if the building with the solar chimney is located in a warm place, when is usual that the external temperature is higher than the comfortable temperature for a building; the height of the chimney is not very important, and will be more effective find solutions to increase the collector area.

4.4 Effect of wind

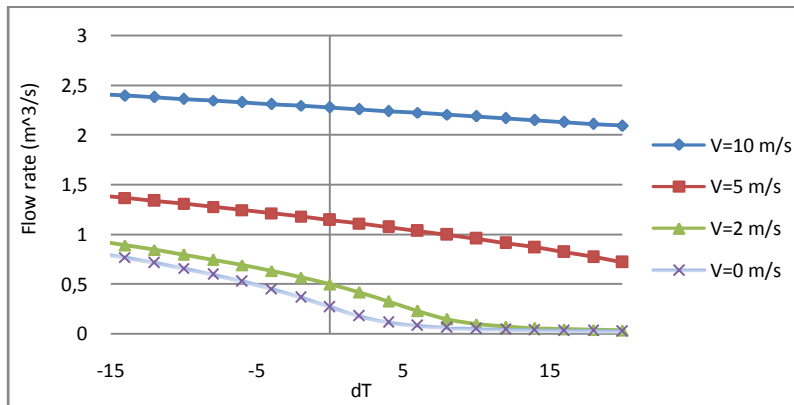
This section studies the effect of the wind in the flow rate across the building and the solar chimney.

To understand better this effect, it has been separated in two parts: the wind velocity and the pressure coefficient

4.4.1 Wind velocity

For the effect of the wind velocity calculations, it has been taken into account a pressure loss coefficient of $C_p=0.25$, like in the work of Cito Oliveira [1]

Figur 4-6 show the effect of the wind velocity in the flow rate. One can see that the effect of velocity increase rapidly with the speed, and for a wind velocity of 5 m/s the effect of the solar chimney can be neglected. Note that, for lower magnitudes of speed (between 1 and 2 m/s) the flow rate increases around 20%; thus the effect of the wind should be taken into account.

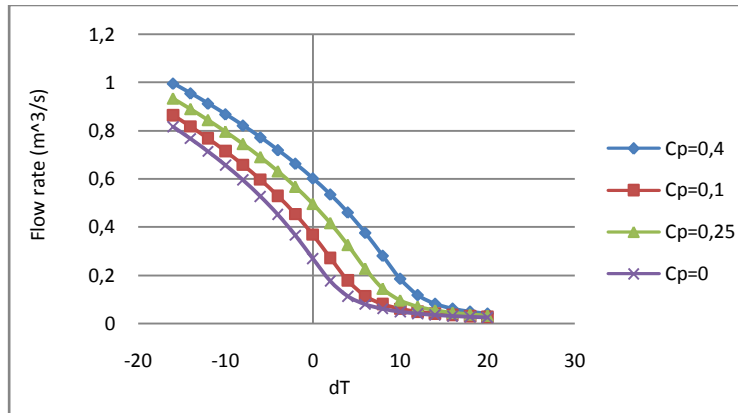


Figur 4-6 Flow rate Vs dT (wind velocity)

4.4.2 Pressure coefficient (Cp)

In this case the wind velocity was set at 2 m/s, because with this speed both effects of wind and solar radiation determine the flow rate.

The value of Cp of a building depends on the direction of the wind, the inlets or openings of the building and the outlet of the chimney [2, 5]. Therefore, the value of Cp is not only a characteristic of the design of the chimney, also depends of the design on the building. The improvements in the Cp in the chimney, only can be make in the design of the outlet using the Venturi effect to make a suction inside the chimney, the problem is that this improvement in the Cp usually increases the drag coefficient of the chimney; thus in the best of the cases the Cp can increase around 0.2 without increase the C_D .



Figur 4-7 rate Vs dT (Cp)

Figur 4-7 shows the effect of the wind pressure coefficient with a constant velocity of 2 m/s. The effect of wind and Cp is more important for a $dT=0$ and $dT>0$ but near to zero, for example when $dT=0$ the flow rate increase around 75% for a $C_p=0,4$ and for $dT=2$ the flow rate increases around 250%. On the other hand if dT is too high the effect of wind is not important. Also when dT decreases the effect of wind decrease smoothly.

4.5 Effect of a heat recovery

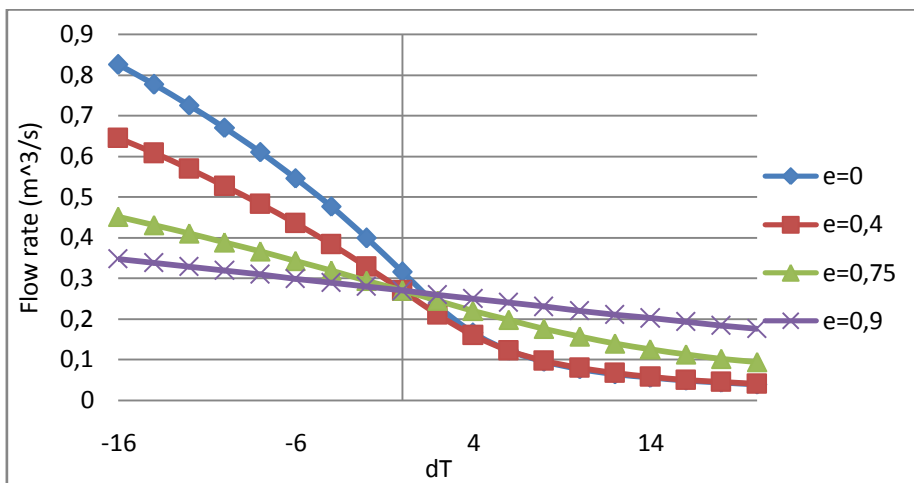
The study or the effect of a heat recovery is motivated for several reasons:

- It has seen previously that the flow rate is greater when the difference of temperature is low ($dT<0$). In the case that the temperature of the room is higher than the comfortable temperature (summer days or in warmer places), the solar chimney helps to remove the extra heat for the building; but on the other hand, when the temperature of the room is lower than the comfortable, the solar chimney increase the heat loss of the building across the building. Therefore even if the efficiency of the chimney increases (more flow rate), the energy efficiency of the building decreases. The use of a heat recovery will help to minimize the heat loss.
- When the temperature of the room is lower than the external, the flow rate is low (Figur 4-2), the use of a heat recovery will help to

heat up the air flow and raise the flow rate, increasing the solar efficiency of the chimney.

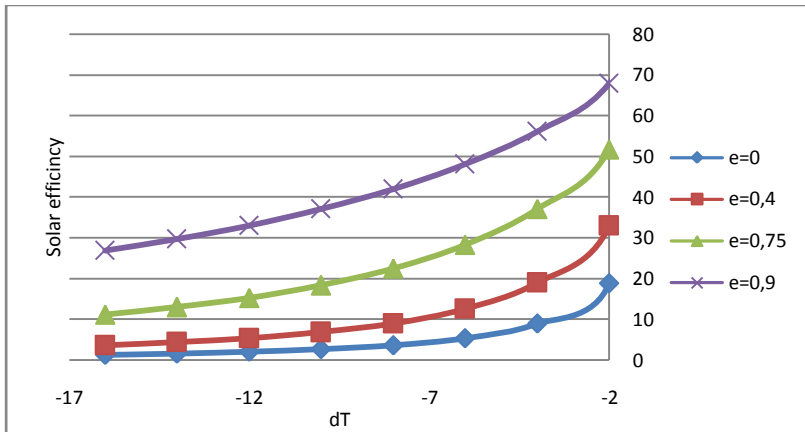
- In buildings with hybrid ventilation (natural and mechanical) is usual to use heat recoveries to improve the energy efficiency.

Three kinds of heat recovery have been studied, one heat pipe with low efficiency ($e=0,4$) [16] and low pressure drop for buildings with natural ventilation, one plate heat exchanger ($e=0,75$) and one heat wheel or cellular recuperator with high efficiency ($e=0,9$) and high pressure drop for hybrid ventilation.



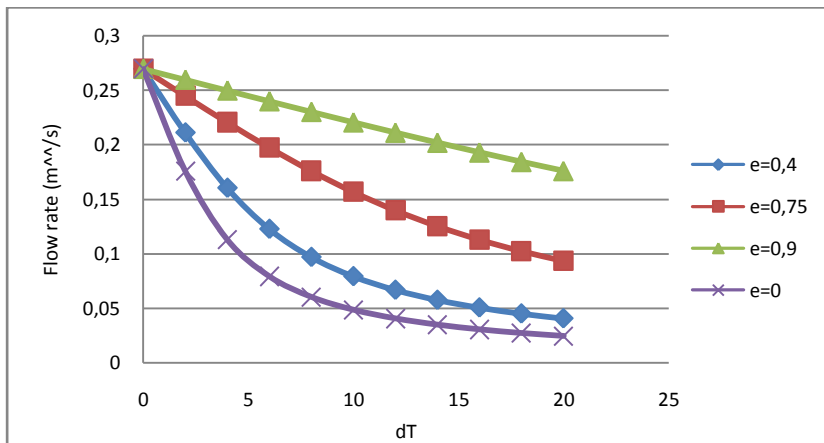
Figur 4-8 Flow rate Vs dT (heat recovery)

As one can expect the flow rate is lower when the efficiency of the heat recovery is higher for $dT < 0$ i.e. the effect of the difference of temperature decrease when it is been used a heat recovery. Figur 4-9 shows this effect.



Figur 4-9 solar efficiency Vs dT (heat recovery)

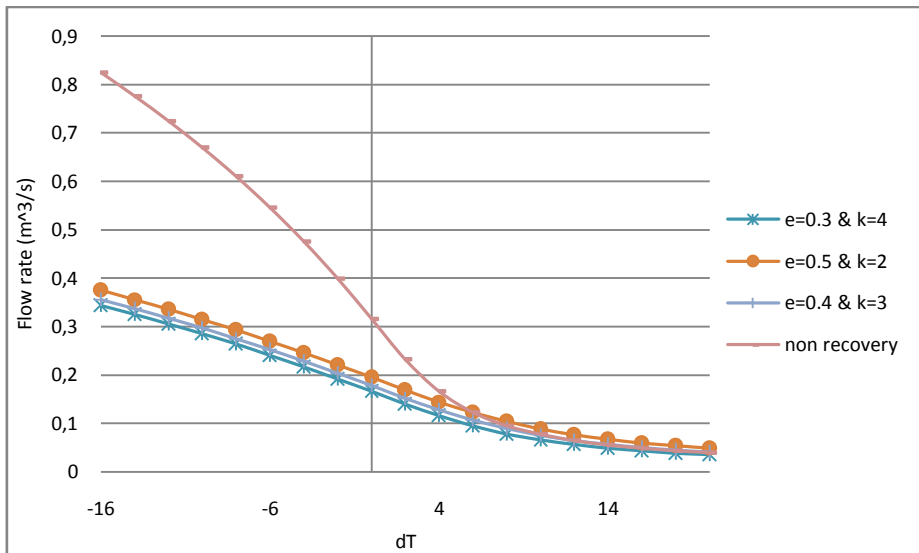
On the opposite, if $dT > 0$, the use of a heat recovery increase the flow rate (Figur 4-10). The use of low efficient heat recover does not improve significantly the ventilation rate, but a normal or high heat recovery will improve substantially the flow rate.



Figur 4-10 Flow rate Vs dT>0 (heat recovery)

These results are not completely realistic because they do not take into account the pressure loss across the heat recovery. Some works [4, 16] demonstrate that for natural ventilation the best option is a heat pipe recovery due to their low pressure drop; also these works give the values of efficiency and pressure loss coefficients for different configurations and flow rate, showing an approximately constant coefficient in function of the air

velocity. The best, the worst and the normal cases was taken to calculate the flow rate in the building and compare without heat recovery.



Figur 4-11 Flow rate Vs dT (heat pipe recovery)

Figur 4-11 shows that a heat recovery with a low pressure drop decreases considerably the air exchange and only, in case when dT is enough high, the heat recovery, make sense to use it. On the other hand, if the building is design with control valve that allows controlling the pass through the heat recovery of the air in function of the difference of temperature; the possibilities of the recuperator increase.

5 Further work

The solar chimney installed in the EPT-lab is a new design and no so much information can be found. Therefore, it is important to continue the work carried out in this Thesis to achieve the design and to understand better the behavior of the solar chimney.

- A 3D CFD simulation with external radiation, to know if the supposition of uniform temperature and velocity can be applied in all angles of incident of solar radiation.
- Verify the equation 3.6 for a range of angles of solar radiation
- Study and simulate different designs of chimney outlets to improve the wind effect in the solar chimney.
- A non-steady simulation of the chimney to know the behavior of the chimney in dynamics conditions, for example the thermal energy storage of the chimney along the day that allows keeping a flow rate during part of the night.

6 Conclusion

This report study the basic principles of solar chimney and especially the chimney installed in EPT-lab, utilizing as tools a commercial CFD software, Fluent, and basic physical models.

The following conclusion could be drawn.

- A simple CFD model, without external radiation is enough to simulated and study with a good accuracy the solar chimney installed in the EPT-lab.
- The design of the solar chimney in the EPT-lab allows to use simple physical models, to know its properties (flow rate and temperature) and also to model the size (height and solar collector area), due to the uniform velocity and temperature that appears inside the chimney. Also these characteristics of the flow make it possible use all the knowledge of the standard chimneys in this solar chimney.
- The EPT- solar chimney can be used in both types of climates (warmer and cold) and for reasonable height it is the type of solar chimney which gives the highest flow rate. Only in warmer climates and in high buildings the solar chimney type 3 will give better results.
- The solar efficiency of the chimney depends of the magnitude of solar radiation, but also of the difference of temperatures between the building and the surroundings. Therefore, only in the cases where the difference of temperature is near to zero, the solar chimney makes sense to use it.
- The height of the chimney is usually important to increase the flow rate, but in the cases when the temperature inside the building is lower than the external it is more important to increase the area of the solar collector than the height of the chimney.
- A solar chimney with a heat recovery improves the solar efficiency of a building but hinders the air exchange. For that reason, only hybrid ventilation systems with the support of a fan and with the enough flexibility to change the course of the flow rate should be used with the solar chimney and a heat recovery.

7 References

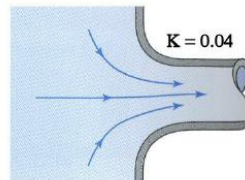
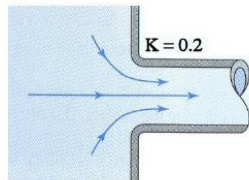
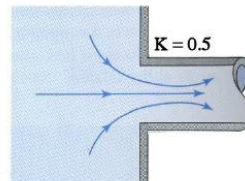
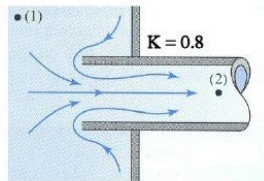
1. Clito Oliveira, A.A., *Solar chimneys: simulation and experiment*. Energy and Buildings, 2000. **32**(1): p. 71-79.
2. Khedari, J., B. Boonsri, and J. Hirunlabh, *Ventilation impact of a solar chimney on indoor temperature fluctuation and air change in a school building*. Energy and Buildings, 2000. **32**(1): p. 89-93.
3. Szikra, C., *Hybrid ventilation systems*. 2002, Budapest University of Technology and Economics.
4. Gan, G. and S.B. Riffat, *A numerical study of solar chimney for natural ventilation of buildings with heat recovery*. Applied Thermal Engineering, 1998. **18**(12): p. 1171-1187.
5. I. Chand and P. Bhargava, *Studies on design and performance of a non-conventional system of natural ventilation in buildings*. Solar and Wind Technology 1990.
6. Ong, K.S., *A mathematical model of a solar chimney*. Renewable Energy, 2003. **28**(7): p. 1047-1060.
7. Sakonidou, E.P., et al., *Modeling of the optimum tilt of a solar chimney for maximum air flow*. Solar Energy, 2008. **82**(1): p. 80-94.
8. Dai, Y.J., et al., *Enhancement of natural ventilation in a solar house with a solar chimney and a solid adsorption cooling cavity*. Solar Energy, 2003. **74**(1): p. 65-75.
9. Agung Murti Nugroho and M.H.b. Ahmad, *POSSIBILITY TO USE SOLAR INDUCED VENTILATION STRATEGIES IN TROPICAL CONDITIONS BY COMPUTATIONAL FLUID DYNAMIC SIMULATION*. 2005: p. 8.
10. Åke Blomsterberg, Åsa Wahlström, and M. Sandberg, *Refurbishment of the Tånga school*. 2002, INTERNATIONAL ENERGY AGENCY, ENERGY CONSERVATION IN BUILDINGS AND COMMUNITY SYSTEMS.
11. Daivid Etheridge and M. Sandberg, *Pressure Differences generated by Temperature*, in *Building Ventilation: Theory and Measurement* 1996. p. 28-29.
12. <http://www.brynmawr.edu/geology/206/gruenstein2.htm>. Solar Tower Technology.
13. http://en.wikipedia.org/wiki/Cubic_function. Cubic function.
14. Carmen Viñas, et al., *Analysis of the Behavior of a Turbulent Jet Indoor*. Informacio Tecnológica, 2008. **19** Nº5: p. 9.
15. ANSYS, I., *ANSYS FLUENT 12.0 Theory Guide*. 2009. 816.
16. Shao, L., S.B. Riffat, and G. Gan, *Heat recovery with low pressure loss for natural ventilation*. Energy and Buildings, 1998. **28**(2): p. 179-184.

17. Störm, H.C., *CFD investigation of flow in and around a natural draft cooling tower*, in *Mechanical and Mechatronic Engineering* 2010.

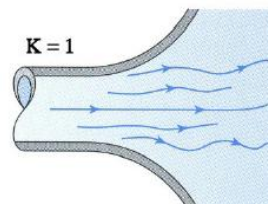
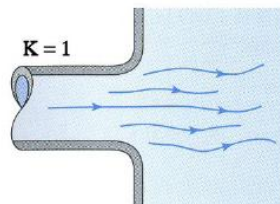
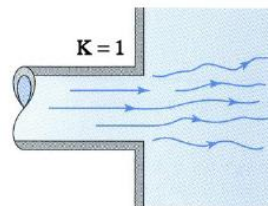
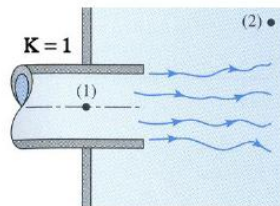
Appendix 1

Pressure Loss Coefficients and Moody Diagram

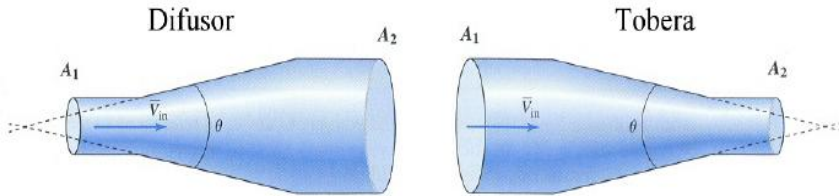
- Inlets



- Outlets

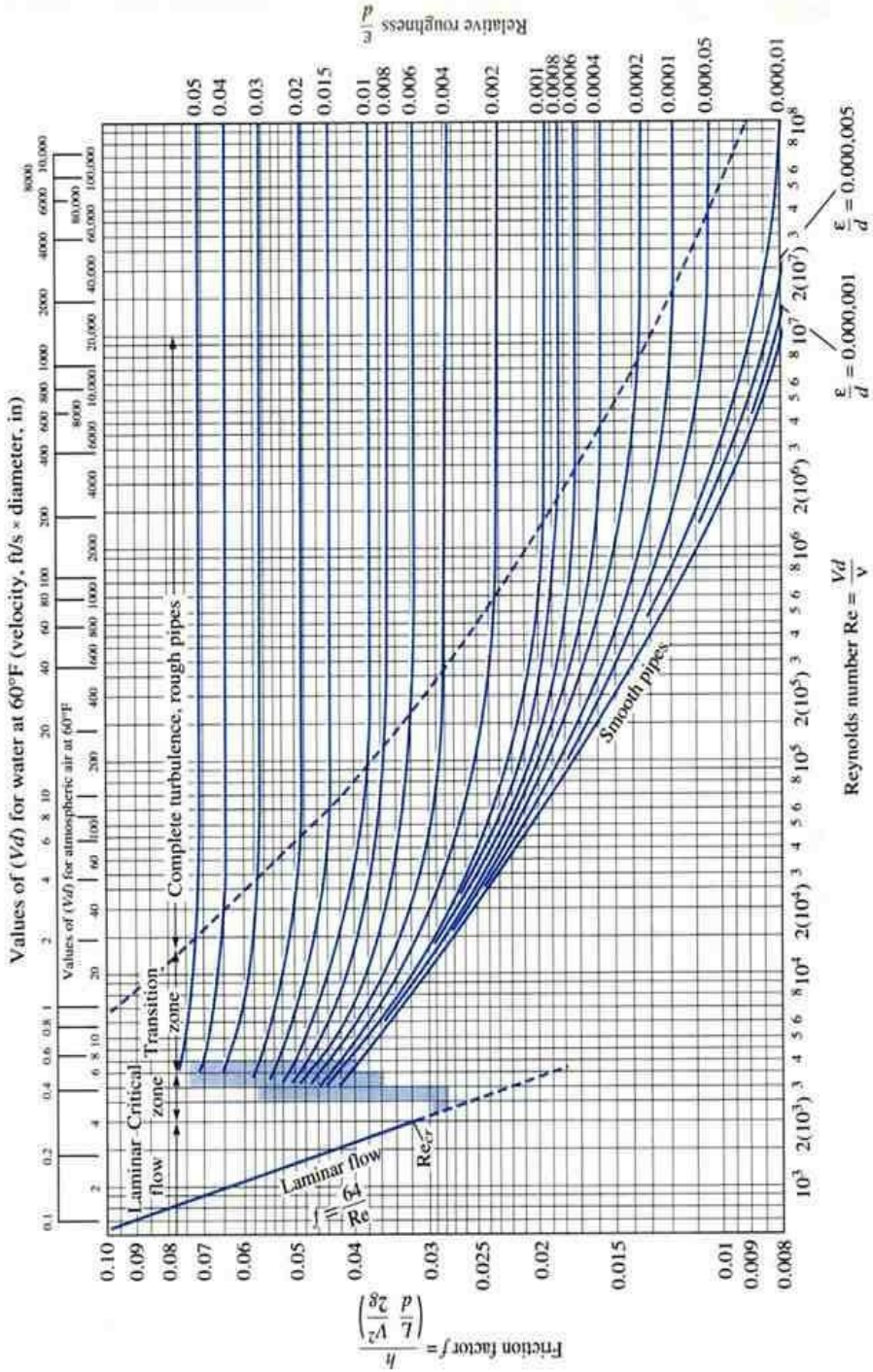


- **Nozzle (Spanish)**
In Spanish nozzle is “tobera”



		Ángulo θ (°)									
A_1/A_2	10	15	20	30	45	60	90	120	150	180	
Coeficiente de pérdida del difusor, K_D											
0.06	0.21	0.29	0.38	0.6	0.84	0.88	0.88	0.88	0.88	0.88	0.88
0.1	0.21	0.28	0.38	0.59	0.76	0.8	0.83	0.84	0.83	0.83	0.83
0.25	0.16	0.22	0.3	0.46	0.61	0.68	0.64	0.63	0.62	0.62	0.62
0.5	0.11	0.13	0.19	0.32	0.33	0.33	0.32	0.31	0.30	0.30	0.30
Coeficiente de pérdida de la tobera, K_T											
1	0	0	0	0	0	0	0	0	0	0	0
2	0.2	0.2	0.2	0.2	0.22	0.24	0.48	0.72	0.96	1	1
4	0.8	0.64	0.64	0.64	0.88	1.1	2.7	4.3	5.6	6.6	6.6
6	1.8	1.4	1.4	1.4	2	2.5	6.5	10	13	15	15
10	5	5	5	5	6.5	8	19	29	37	43	43

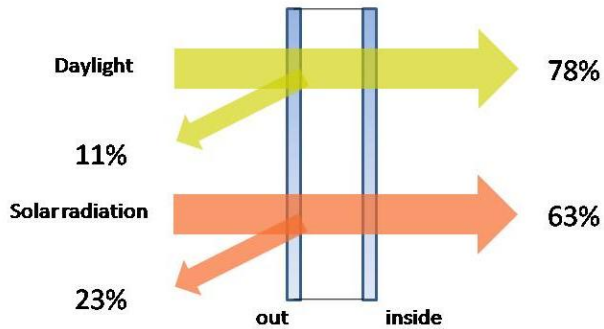
- Moody Diagram



Appendix 2

Window data

$U_g=1,2W/m^2K$

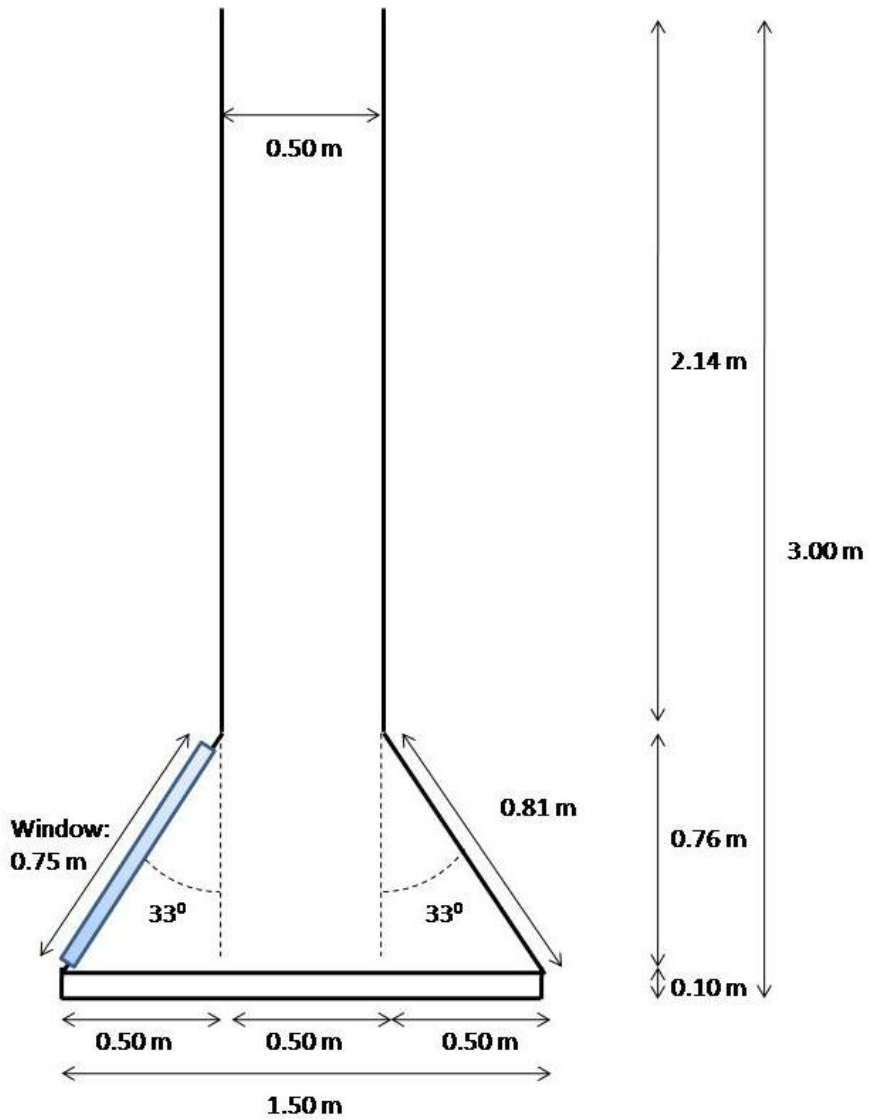


Position outside	Glass type	Thickness mm	Weight kg/m ²
Glass 1	Optifloat™ Clear	4	10
Space	90% Argon		
Glass2	Optitherm™ SN	15	10
	Product code	Type	Thickness mm
	4-15Ar-SN4	2	23
			Weight kg/m ²
			20

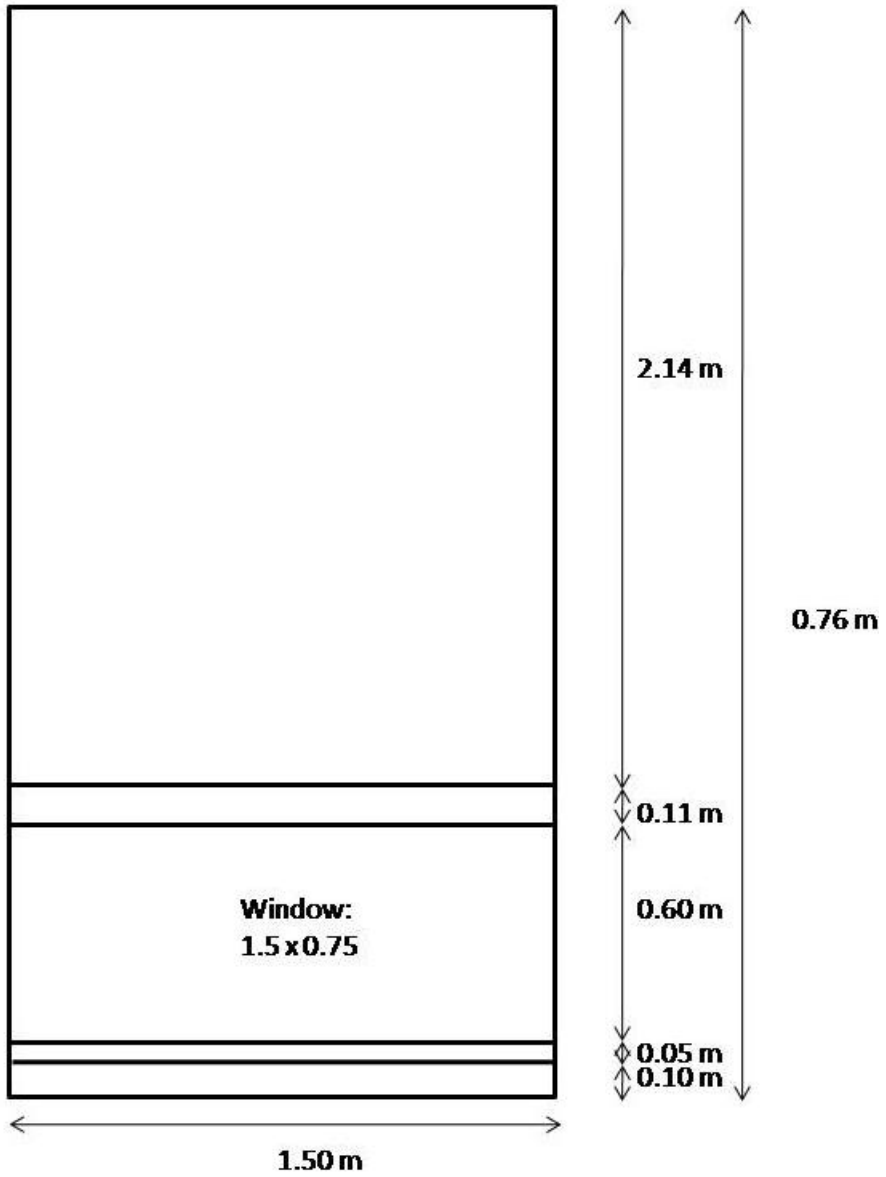
Appendix 3

Solar Chimney EPT-lab

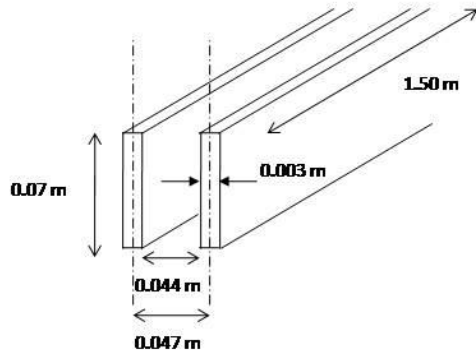
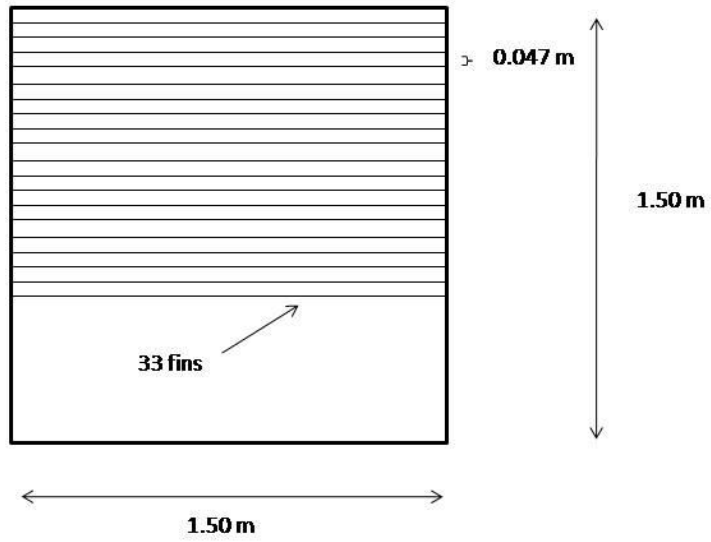
- Chimney side



- Chimney front

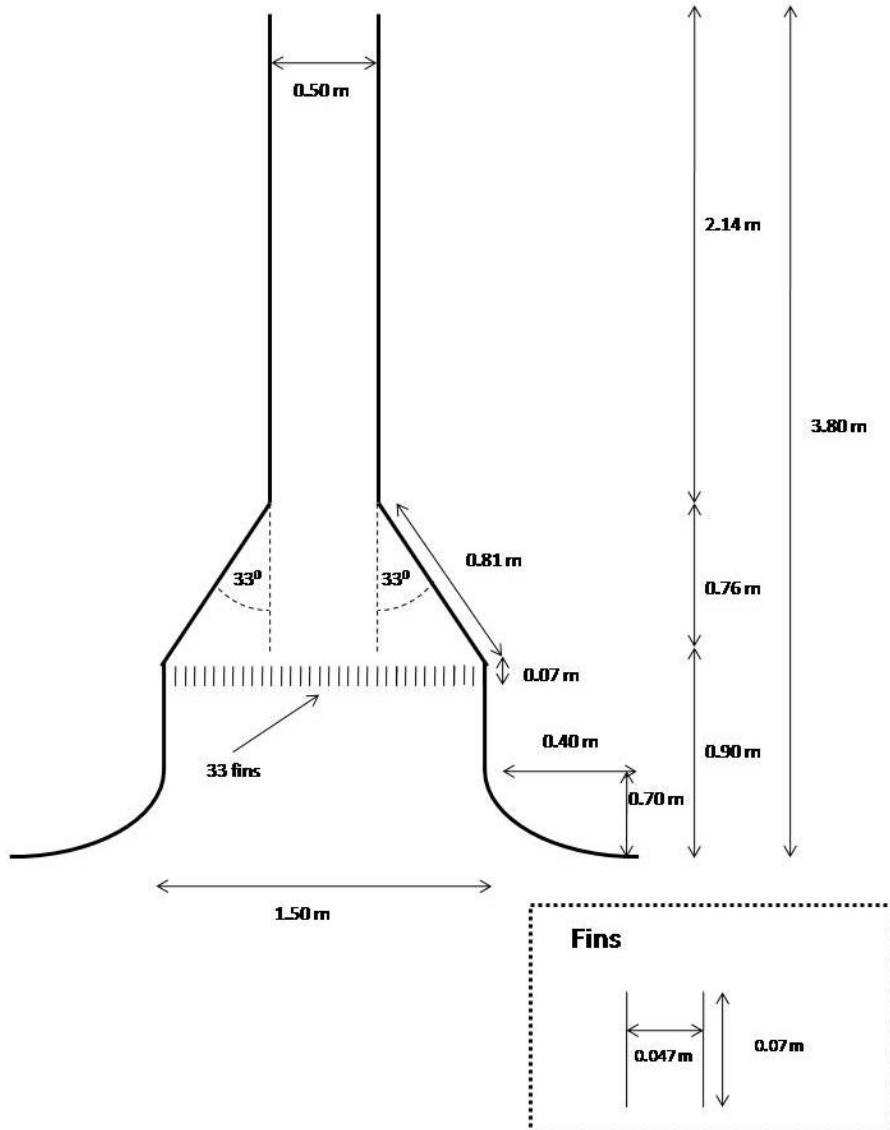


- Sola collector and fins



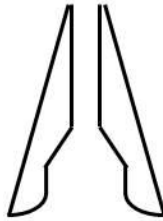
Appendix 4

CFD Solar Chimney Model



Pressure outlet:

Back flow conditions: $T=300K$, $k=1$ and $e=0.3$



Slip conditions $T=300K$

$V=0.01m/s$ $T=300K$

$K=1$ $e=0.3$